THE JOURNAL OF BIOLOGICAL CHEMISTRY VOL. 287, NO. 8, pp. 5492–5506, February 17, 2012

Decorin Antagonizes the Angiogenic Network

CONCURRENT INHIBITION OF MET, HYPOXIA INDUCIBLE FACTOR 1α, VASCULAR ENDOTHELIAL GROWTH FACTOR A, AND INDUCTION OF THROMBOSPONDIN-1 AND TIMP3[*][S]

Received for publication, July 16, 2011, and in revised form, December 5, 2011 Published, JBC Papers in Press, December 22, 2011, DOI 10.1074/jbc.M111.283499

Thomas Neill[‡1], **Hannah Painter**[‡], **Simone Buraschi**[‡], **Rick T. Owens**[§], **Michael P. Lisanti**[¶], **Liliana Schaefer**[‖], **and Renato V. Iozzo**[‡2]

From the [‡]*Department of Pathology, Anatomy and Cell Biology, the Cancer Cell Biology and Signaling Program, and the* [¶]*Stem Cell Biology and Regenerative Medicine Center, Kimmel Cancer Center, Thomas Jefferson University, Philadelphia, Pennsylvania 19107,* [§]*LifeCell Corporation, Branchburg, New Jersey 08876, and the* [‖]*Goethe University, Frankfurt 60590, Germany*

Background: Decorin antagonizes multiple receptor tyrosine kinases, such as Met, to suppress tumorigenesis.
Results: Decorin promotes angiostasis by blocking hypoxia inducible factor-1α and β-catenin to inhibit vascular endothelial growth factor A and matrix metalloprotease-2/9 activity concurrent with thrombospondin-1 and TIMP3 induction.
Conclusion: Decorin abrogates the pro-angiogenic HGF/Met signaling axis, thereby repressing vascular endothelial growth factor A-mediated angiogenesis under normoxia.
Significance: Soluble decorin attenuates early tumor growth by preventing normoxic angiogenic signaling through the Met receptor.

Decorin, a small leucine-rich proteoglycan, inhibits tumor growth by antagonizing multiple receptor tyrosine kinases including EGFR and Met. Here, we investigated decorin during normoxic angiogenic signaling. An angiogenic PCR array revealed a profound decorin-evoked transcriptional inhibition of pro-angiogenic genes, such as *HIF1A*. Decorin evoked a reduction of hypoxia inducible factor (HIF)-1α and vascular endothelial growth factor A (VEGFA) in MDA-231 breast carcinoma cells expressing constitutively-active HIF-1α. Suppression of Met with decorin or siRNA evoked a similar reduction of VEGFA by attenuating downstream β-catenin signaling. These data establish a noncanonical role for β-catenin in regulating VEGFA expression. We found that exogenous decorin induced expression of thrombospondin-1 and TIMP3, two powerful angiostatic agents. In contrast, decorin suppressed both the expression and enzymatic activity of matrix metalloprotease (MMP)-9 and MMP-2, two pro-angiogenic proteases. Our data establish a novel duality for decorin as a suppressor of tumor angiogenesis under normoxia by simultaneously down-regulating potent pro-angiogenic factors and inducing endogenous anti-angiogenic agents.

A pertinent concept in the field of tumorigenesis is the critical role of the extracellular matrix as an active participant in the regulation of diverse cell processes and signaling events that form an environment signified by ever changing flux (1). These diverse cellular processes, permissive for tumor progression, are often modulated by matrix constituents that culminate to affect tumor invasion, metastasis, and angiogenesis (2).

Various members of the proteoglycan gene family are intimately involved in regulating tumor angiogenesis by directly affecting key downstream signaling pathways via interaction with ligands and their cognate receptors (3–5). Decorin, a prototypical member belonging to a superfamily of 18 individually encoded gene products collectively known as the small leucine-rich proteoglycans (6–8), has been implicated in regulating angiogenesis.

Decorin was originally characterized to bind fibrillar collagen, primarily type I, and to regulate fibrillogenesis (9–16), tissue mechanical properties (17–21), and wound healing and fibrosis (22, 23). Decorin also regulates the entry of *Borrelia burgodferi* spirochetes, the causative agent of Lyme disease, into the dermis (24, 25) and several other pathophysiological processes including dentin and bone mineralization (26–28), skeletal muscle homeostasis (29), vertebrate convergent extension (30), bone marrow stromal cell fate (31), myocardial infarction (32), corneal transparency (33), various types of nephropathies (34–38), and tumor inflammation (39).

In the context of cancer, decorin was first identified as a proteoglycan highly induced in the stroma of colon cancer (40, 41) suggesting that decorin might counteract the growth of malignant cells in a paracrine fashion. Subsequently, it was discovered that decorin evokes down-regulation of multiple receptor tyrosine kinases (RTKs)[3] including the EGFR (42–45) as well as to other ErbB family members (46). This signaling leads to

* This work was supported, in whole or in part, by National Institutes of Health Grants RO1 CA39481, RO1 CA47282, and RO1 CA120975 (to R. V. I.).
[S] This article contains supplemental Table S1 and Figs. S1–S6.
[1] Supported by National Institutes of Health Training Grant T32 AA07463. This work is in partial fulfillment of a doctoral thesis in Cell and Developmental Biology, Thomas Jefferson University.
[2] To whom correspondence should be addressed: 1020 Locust St., Rm. 249 JAH, Thomas Jefferson University, Philadelphia, PA 19107. Tel.: 215-503-2208; Fax: 215-923-7969; E-mail: iozzo@kimmelcancercenter.org.

[3] The abbreviations used are: RTK, receptor tyrosine kinase; EGFR, epidermal growth factor receptor; HGF, hepatocyte growth factor; VEGFA, vascular endothelial growth factor A; HIF-1α, hypoxia inducible factor 1α; CDKI, cyclin-dependent kinase inhibitor; qPCR, quantitative real-time polymerase chain reaction; MMP, matrix metalloprotease; HUVEC, human umbilical vein endothelial cell; pVHL, protein Von Hippel-Lindau.

marked tumor growth inhibition (47), induction of the cyclin-dependent kinase inhibitor $p21^{WAF1/Cip1}$ (p21) (48, 49) and mobilization of intracellular Ca^{2+} stores in cancer cells (50). Moreover, decorin has been found to antagonize the Met proto-oncogene (51) by receptor internalization via caveolar-mediated endocytosis (52), resulting in cessation of signaling analogous to EGFR (53). This mode of action is in stark contrast to clathrin-mediated endocytosis of Met (54), which enables Met to maintain a prolonged activation of downstream signaling (55).

Although decorin-null mice are apparently normal (9), double mutant mice lacking decorin and p53 succumb very early to very aggressive lymphomas suggesting that loss of decorin is permissive for tumorigenesis (56). This concept is further corroborated by a recent study using decorin-null mice in a different genetic background. Under these conditions, lack of decorin causes intestinal tumor formation, a process exacerbated by exposing the mice to a high-fat diet (57). Conversely, delivery of the decorin gene or protein retards the growth of a variety of cancers (58–65).

The role of decorin in tumor angiogenesis is controversial. Previous reports have delineated a pro-angiogenic response, primarily on normal, nontumorigenic endothelial cells (66–68) or through loss of decorin in the cornea (69). Interestingly, an anti-angiogenic role for decorin has also been described in various settings (70–72) and as an angiostatic agent targeting tumor cells, which exhibit dysregulated angiogenesis via a reduction in vascular endothelial growth factor (VEGF) production (73). The apparent dichotomous effects reported for decorin on endothelial cells and the perceived function on the tumor itself creates a scenario where decorin is able to differentially modulate angiogenesis. This is further substantiated by a recent report where the expression of decorin was evaluated as a function of tumor malignancy. Sarcomas exhibited almost a complete absence of decorin in contrast to hemangiomas, where decorin was predominantly detected in the surrounding stroma (74). Aside from the potent pro-migratory, pro-invasive, and pro-survival roles inherent with aberrant Met activation (75), the Met signaling axis is powerfully pro-angiogenic, specifically promoting VEGFA-mediated angiogenesis (76, 77). These observations coupled to the discovery of rapid and sustained physical down-regulation of Met evoked by nanomolar concentrations of recombinant decorin (51, 52) led us to hypothesize that decorin could inhibit angiogenesis via down-regulation of the Met signaling axis.

In the present study, we provide mechanistic insight supporting a functional link between decorin and the Met signaling axis, *vis á vis* the regulation of pathological VEGF-mediated angiogenesis. The angiostatic effects resulting in a marked inhibition of VEGFA occur at both the transcriptional and post-transcriptional levels with upstream signaling occurring via Met, which is antagonized by decorin. Furthermore, our findings indicate a novel induction of thrombospondin-1 and TIMP3, coincident with the suppression of pro-angiogenic molecules. Thus, our data reinforce and extend the critical role for decorin as an antagonist of tumor angiogenesis.

EXPERIMENTAL PROCEDURES

Cells and Materials—HeLa squamous carcinoma and MDA-MB-231 triple-negative breast carcinoma cells were obtained from American Type Culture Collection (Manassas, VA). MDA-MB-231 (hereafter referred to as MDA-231 including derivative MDA-231 cell lines), MDA-231(GFP^+), wtHIF-1α, and mutHIF-1α cells were previously described (78). Cells were maintained in Dulbecco's modified Eagle's medium supplemented with 10% fetal bovine serum (FBS) (SAFC Biosciences, Lenexa, KS) as well as with 100 μg/ml of penicillin/streptomycin (MediaTech, Manassas, VA). Human umbilical vein endothelial cells (HUVECs) were purchased from Lifeline Cells Technology (Walkersville, MD) and used only within the first 5 passages. Primary antibodies against VEGFA (sc-152) and Met (Met-C12, Sc-10) were from Santa Cruz Biotechnology (Santa Cruz, CA); rabbit polyclonal anti-β-catenin (ab16051) and anti-MMP-14 (ab3644) antibodies were purchased from Abcam Inc. (Boston, MA); mouse monoclonal anti-β-actin antibody was from Sigma. The anti-perlecan antibody has been previously characterized (79, 80).

Slot Blot Assay for Analysis of Secreted VEGFA—Cells were treated with decorin protein core in DMEM for 24 h. Conditioned medium was collected, filtered, then briefly centrifuged and applied to the slot blot sample acceptor. Suction was applied for 30 min to ensure attachment to the nitrocellulose membrane, which was washed and blocked overnight. Incubation with a primary antibody specific for the secreted factor was followed by application of an infrared-labeled secondary antibody and subsequent visualization and quantification via the Odyssey Infrared System.

Transient Knockdown of Met Receptor—Transient knockdown of the Met receptor was achieved via utilization of a mixture consisting of three validated siRNAs specific for Met mRNA (Met siRNA sc-29397 Santa Cruz). Briefly, six-well plates were seeded with 2×10^5 HeLa cells, followed by incubation overnight at 37 °C until cultures were 70% confluent. Targeting siRNA duplex at a final concentration of 80 pM was added to diluted Lipofectamine 2000 (Invitrogen) in Opti-MEM I Reduced Serum Medium (Invitrogen). Transfection was carried out for 48 h at 37 °C and the cells were then treated with DMEM or decorin (500 nM) for an additional 24 h. Verification of siRNA-mediated knockdown of the Met receptor was determined via immunoblotting using Met-specific antibodies.

Quantitative Real Time-PCR Analysis—Gene expression analysis by quantitative real time-polymerase chain reaction (qPCR) was carried out as described before (81) with minor modifications. Briefly, subconfluent ($\sim 1.5 \times 10^6$ cells) 3.5-cm^2 dishes of HeLa cells were treated for 24 h with either PBS (mock) or 500 nM decorin protein core in DMEM. After incubation, cells were lysed directly in 500 μl of TRIzol reagent (Invitrogen). Tumor RNA was obtained as described before (52). Subsequent isolation of RNA and cDNA synthesis proceeded as for cell culture. As such, total RNA (1 μg) was annealed with oligo(dT) primers and cDNA was synthesized utilizing the SuperScript Reverse Transcriptase II (Invitrogen) according to the manufacturer's instructions. Gene-specific primers were verified before use (supplemental Table S1). The

target genes and endogenous housekeeping gene (*ACTB*) amplicons were amplified in independent reactions using the Brilliant SYBR Green Master Mix II (Agilent Technologies, Cedar Creek, TX). All samples were run in quadruplicate on an Mx3005P Real Time PCR platform (Agilent) or on a LightCycle 480-II (Roche Applied Science) and the cycle number (C_t) was obtained for each independent reaction. Fold-change determinations were made utilizing the comparative C_t method for gene expression analysis. Briefly, ΔC_t values are representative of the normalized gene expression levels with respect to *ACTB* (β-actin as the endogenous housekeeping control). $\Delta\Delta C_t$ values represent the experimental cDNA (samples treated with 500 nM decorin protein core) minus the corresponding gene levels of the calibrator sample (samples treated with PBS mock). Finally, the reported fold-change represents an average of the fold-changes as calculated using the double ΔC_t method ($2^{-\Delta\Delta CT}$). Data were derived from 2 to 3 independent trials for each gene of interest.

RT^2 Profiler PCR Array—The specific expression of angiogenic genes was evaluated using a human RT^2 *Profiler*™ PCR Array (SABiosciences), which contained primers for the detection of 84 different known angiogenic genes. This analysis was carried out according to the manufacturer's instructions. Briefly, subconfluent 3.5-cm^2 dishes of HeLa cells were treated for 24 h with either PBS (vehicle) or 500 nM decorin protein core in DMEM. After incubation, the cells were lysed directly in TRIzol reagent (Invitrogen) for subsequent RNA isolation. Total RNA was reverse transcribed to cDNA using the RT^2 First Stand Kit (SABiosciences) followed by combination with the RT^2 qPCR Mastermix. This volume was evenly distributed among two PCR array plates. Consecutive rounds of qPCR were performed under normal thermal conditions followed by data analysis according to the above mentioned C_t method post-normalized to five independent controls.

Immunofluorescence—Immunofluorescent studies were performed as described before (53, 82, 83). Approximately 5×10^4 HeLa cells were plated on 4-well chamber slides (BD Biosciences) and grown to full confluence in 10% FBS at 37 °C. Cells were switched to DMEM, 2% FBS 2 h prior to each treatment. Slides were rinsed twice with Dulbecco's phosphate-buffered saline and fixed/permeabilized with ice-cold methanol for 10 min. Subsequently slides were subjected to standard immunofluorescence protocols, and mounted with Vectashield (Vector Laboratories Inc., Burlingame, CA). Following incubation with various primary antibodies, detection was determined using goat anti-mouse IgG Alexa Fluor® 488 and goat anti-rabbit IgG Alexa Fluor® 594 (Invitrogen). Images were acquired using a Leica DM5500B microscope with Advanced Fluorescence 1.8 software (Leica Microsystems, Inc.). All the images were analyzed with Adobe Photoshop CS3 (Adobe Systems, San Jose, CA). Fluorescence quantification was done with ImageJ software.

Gelatinase Zymography—Gelatinase activities evaluated in tumor-conditioned medium (10 μl) collected from HeLa cells after incubation with 500 nM decorin for a period of 24 h were quantified with 10% SDS-PAGE incorporating denatured rat tail type I collagen (Sigma) (84). The sample buffer did not contain reducing agents. Gels were washed in 2.5% (v/v) Triton X-100 (1 h at room temperature) and incubated overnight in 50 mM Tris-HCl, pH 7.6, 0.1 mM NaCl, 10 mM $CaCl_2$, 0.05% Brij in the presence or absence of 20 mM EDTA (all from Sigma). Enzymatic activity was visualized as negative staining with Coomassie Brilliant Blue R-250 (Sigma) and quantified using Quantity One One-dimensional Analysis Software (Bio-Rad). The results of six samples per group were averaged.

Quantification of Matrix Metalloprotease (MMP) Levels—The detection of total MMP-9 and MMP-2 present in tumor-conditioned medium was carried out by ELISA according to the individual kits assaying Human MMP-9 and Human MMP-2 Immunossay Quantikine Colorimetric Sandwich ELISA (R&D Systems, Minneapolis, MN) according to the manufacturer's protocol. These assays employ a quantitative sandwich ELISA technique via a monoclonal antibody specific for both the 92-kDa pro-MMP-9 (gelatinase B) as well as the 82-kDa active MMP-9. Detection of human MMP-2 (gelatinase A) via the Human MMP-2 Quantikine kit was performed with a polyclonal antibody cognant for the 72-kDa MMP-2. Briefly, tumor-conditioned medium samples generated by a subconfluent 6-well plate of HeLa cells, previously treated with either PBS (mock control) or decorin protein core (500 nM) for 24 h, were collected. The precoated plates received assay diluent followed by application of standard, control, and sample cell medium aliquots followed by a 2-h incubation at 25 °C. The plates were washed extensively, incubated with the substrate for 30 min, and read at 450 nm.

Evaluation of mRNA Stability—Determination of mRNA decay processes were evaluated in HeLa cells via pre-treatment of actinomycin D (Sigma) for 1 h followed by treatment (4 h) with decorin core protein (100 and 500 nM). At the conclusion of the experiment, medium was aspirated, cells were washed in PBS and lysed in TRIzol for RNA isolation and cDNA synthesis (see above protocol). The cDNA was subsequently analyzed via qPCR (see the above protocol for workflow and $\Delta\Delta C_t$ methodology) to evaluate the resulting non-steady state mRNA levels of selected target genes in the presence or absence of decorin.

MMP-9 Functional Assay—Evaluation of endogenous MMP-9 activity present in HeLa-conditioned medium in the absence or presence of decorin core protein (500 nM) was carried out via utilization of the SensoLyte® Plus 520 MMP-9 Assay Kit (AnaSpec, San Jose, CA) (85, 86). Briefly, following the 24-h incubation with decorin, tumor-conditioned DMEM was collected, filtered (0.2 μm), and centrifuged. The supernatant was subsequently used to generate 2-fold dilutions (up to and including 1:128). About 100 μl of each dilution was added to each microplate well, which contained a pre-coated monoclonal anti-human MMP-9 antibody. Pulldown (1 h at 25 °C) of endogenous MMP-9 was succeeded by activation of the pro-MMP-9 present only in the standard curve with 1 mM *p*-aminophenylmercuric acetate for 2 h at 37 °C but not for the control or experimental samples. This allowed direct evaluation of endogenously active MMP-9 in the applied samples. Next, active MMP-9 activity was assayed via the addition of the synthetic MMP-9 5-FAM/QXL520 FRET peptide. Following an 8-h incubation with this MMP-9 substrate, end point analysis was determined by measuring the fluorescence intensity, which measures the activity of MMP-9, on a BioTek Synergy 4 plate

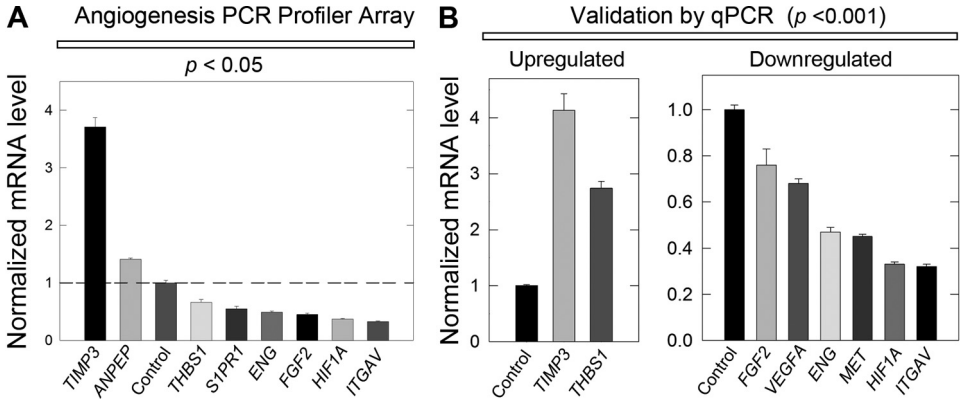

FIGURE 1. **Decorin inhibits VEGFA-mediated angiogenesis by attenuating pro-angiogenic factors.** *A,* RT^2 PCR Profiler Angiogenesis Array evaluating pro-angiogenic gene expression changes in HeLa cells following exposure to 500 nM decorin after 24 h. *B*, PCR array target gene verification performed via qPCR under the same conditions as in *A*. PCR Profiler Angiogenesis Array and all subsequent qPCR verification analyses were performed in triplicate among three independent experiments, normalized to the endogenous housekeeping gene, *ACTB,* and reported as average fold-changes ± S.E. in agreement with the comparative $\Delta\Delta C_t$ method (please see "Experimental Procedures" for a full and detailed description).

reader (BioTek Instruments, Winooski, VT) at an emission/excitation of 490/520 nm.

Tumor Xenograft Matrigel Plug Assays—Approximately 80 μl of Matrigel™ (BD Biosciences) containing ~10^6 MDA-231(GFP$^+$) cells and hepatocyte growth factor (HGF) (10 ng/ml), in the presence or absence of decorin (200 nM), were injected into 4 dorsal subcutaneous regions of 6 severe combined immunodeficient, nude, female mice (Charles River Laboratories). Mice were sacrificed 14 days post-injection and their skins were removed, fixed in 10% buffered formalin (Fisher Science, Fair Lawn, NJ), and then photographed from the inside to analyze the resulting angiogenic reaction. Quantification was achieved by ImageJ software and superimposing grids onto each photographed skin with each box of the grid representing 1 mm^2. Fifty, randomly selected boxes around each Matrigel plug were analyzed by morphometry. That is, the number of times a blood vessel intersected each box was recorded for both "Matrigel + HGF" and "Matrigel + HGF + decorin." Values were converted into μm^2 and a Student's two-sided *t* test (see below) was used to compare the values obtained from the control and experimental conditions.

Tumor Xenografts—All animal studies were approved by the Institutional Review Board of Thomas Jefferson University. For orthotopic mammary tumor xenografts, severe combined immunodeficient female mice (Charles River Laboratories) were injected in the upper left mammary glad with 1–2 × 10^6 MDA-231(GFP$^+$) cells. The mice were randomized once tumors were established. Half of the mice received a dose of 5 mg/kg of decorin protein core injected intraperitoneally every 2 days. The controls received 100 μl of PBS. On day 24, the majority of animals were sacrificed and all major organs and tumors were dissected and frozen subsequent to analysis via immunofluorescence or qPCR. HeLa xenografts were generated as described before (52).

Dot Blot Analyses of Secreted Factors—Evaluation of secreted factors was done, in part, via dot blot analysis. HeLa and MDA-231 cells were treated as described under serum-free conditions (see below). Tumor cell-conditioned medium was collected, filtered, briefly centrifuged, and applied to the dot blot (Minifold I, Schleicher and Schuell, Keene, NH) sample well plate. Constant vacuum (~80 mbar) was applied for 30 min to ensure attachment to the nitrocellulose membrane. The membrane was washed and blocked overnight in 5% BSA. Incubation with primary antibody specific for the secreted factor was followed by application of an HRP-conjugated secondary antibody and subsequent visualization with ECL. Densitometry was performed with ImageJ software.

Quantification and Statistical Analysis—Immunoblots were quantified by scanning densitometry using ImageJ software or using the Odyssey software for the infrared-labeled secondary antibodies. All experiments were carried out in triplicate and repeated at least three times. Results are expressed as mean ± S.E. Statistical analysis was performed with SigmaStat for Windows version 3.10 (Systat Software, Inc., Port Richmond, CA). Significance of differences was determined by unpaired Student's *t* test. Statistical significance was achieved with $p < 0.05$. For quantification of immunofluorescence studies, fluorescence intensity and three-dimensional surface plots were quantified by measuring pixels with ImageJ software as described before (52).

RESULTS

Decorin Broadly Impedes the Transcription of Pro-angiogenic Genes and Up-regulates the Expression of Angiostatic Genes—First, we determined the effects of decorin on the expression of angiogenic genes using a human RT^2 *Profiler*™ PCR Array (SABiosciences). This PCR array platform profiles the expression of 84 key genes involved in modulating the biological processes of angiogenesis, including growth factors and their receptors, chemokines and cytokines, matrix and adhesion molecules, proteases, as well as transcription factors.

To this end, HeLa cells were treated for 24 h in the absence or presence of 500 nM decorin protein core under normoxic conditions whereupon total RNA was harvested, reverse transcribed to cDNA libraries, and then applied to the cognate PCR array plates. Normalization of raw C_t values to five endogenous controls allowed for a comparative $\Delta\Delta C_t$ analytic approach between calibrator samples (PBS control) and experimental (decorin) samples. First, only ~10% of all genes were changed: two were up-regulated and six were down-regulated by decorin

(Fig. 1*A*). Notably, *TIMP3* was induced over 4-fold by decorin and this product has been previously shown to be anti-angiogenic (87). The six down-regulated genes (Fig. 1*A*), including hypoxia inducible factor-1α (*HIF1A*), sphingosine 1-phosphate receptor 1 (*S1PR1*), endoglin (*ENG*), fibroblast growth factor 2 (*FGF2*), and integrin αV (*ITGAV*), were all quite interesting because all have been implicated in promoting key aspects of angiogenic signaling (88–94), with the notable exception of thrombospondin-1 (*THBS1*), which has been shown to exhibit potent anti-angiogenic activities (95, 96).

Next, we validated the modulated genes using qPCR (Fig. 1*B*). The great majority of the transcriptional changes reported by the PCR Array were reliably reproduced. However, the expression changes for aminopeptidase-N (*ANPEP* or *CD13*) and *S1PR1* could not be reproduced and validated most likely reflecting either an exceedingly low transcript copy number or sheer lack of expression in HeLa cells. Notably, thrombospondin-1, a well known anti-angiogenic factor (95, 96) was found to be slightly down-regulated in the presence of decorin (Fig. 1*A*). However, verification of this gene via qPCR revealed *THBS1* to be significantly up-regulated by ~2.5-fold ($p < 0.001$, Fig. 1*B*). Additional pro-angiogenic gene targets found to be repressed by decorin included VEGFA and Met. Because we normalized C_t values to endogenous *ACTB* in each sample, we conducted qPCR to ensure the expression of this housekeeping gene was not affected by exogenous decorin. Thus, after 24 h we found that *ACTB* (supplemental Fig. S1*A*) in HeLa was not significantly modulated by decorin (500 nM). Furthermore, we sought to determine *ACTB* over time and demonstrate that up to 8 h in HeLa, *ACTB* mRNA levels also did not significantly change (supplemental Fig. S1*B*). Therefore, we conclude the changes seen in target gene expression are not a result of β-actin modulation at the mRNA level.

The expression changes were done at steady state kinetics but could alternatively represent the effects of decorin on modulating mRNA stability and/or accelerating decay processes of the target message. To address this possibility, we evaluated *VEGFA, HIF1A,* and *THBS1* in the presence of decorin following pre-treatment with actinomycin D in HeLa. We found no further changes in mRNA for *VEGFA* (supplemental Fig. S1*C*), *HIF1A* (supplemental Fig. S1*D*), or *THBS1* (supplemental Fig. S1*E*), indicating that decorin does not modulate mRNA levels post-transcriptionally by promoting mRNA decay. We can thus conclude that the changes seen at the steady state reflect a decrease at the level of transcription.

Collectively, these expression data implicate decorin as a broad suppressor of the tumor angiogenic response by exhibiting a unique duality. It effectively represses pro-angiogenic gene targets under normoxia and simultaneously promotes the expression of various anti-angiogenic effector molecules.

Exogenous Decorin Potently Attenuates VEGFA Signaling Components—Among the down-regulated genes reported in the expression analysis above, we chose to focus on the VEGFA signaling axis as it relates to tumor angiogenesis. First, we determined whether the activity of decorin could be generalized to normal as well as transformed cells. Thus, we tested two tumor cell lines and normal endothelial cells for the effects of exogenous decorin on VEGFA production. Following decorin exposure, we found a uniform reduction of secreted VEGFA in the medium conditioned for 24 h by HeLa (cervical carcinoma) and MDA-231 (triple-negative breast carcinoma) cells as well as from HUVECs ($p < 0.001$, Fig. 2, *A* and *B*).

The reduced levels of VEGFA found in the conditioned medium could be a consequence of a corresponding decrease in total cellular stores of VEGFA or an inhibitory effect of VEGFA secretion. To differentiate among these possibilities, we probed cell lysates using immunoblotting with the same anti-VEGFA antibody. We found a decrease in cellular VEGFA in both HeLa and MDA-231 and to a lesser extent in HUVECs ($p < 0.001$ and < 0.01, respectively, Fig. 2, *C* and *D*). The difference in sensitivities among these cell lines are attributable to higher Met in HeLa and MDA-231 (6- and 8-fold higher, respectively) relative to HUVEC (data not shown). Enhanced expression of this high affinity receptor would further sensitize the cells to the angiostatic properties of decorin.

Next, we found a significant reduction of both secreted and cellular VEGFA (supplemental Fig. S2, *A* and *B*) after 24 h in HeLa and MDA-231 following decorin treatment (100 nM). Thus, a concentration of 100 nM is sufficient to evoke reduction of secreted and cellular VEGFA.

Time course experiments utilizing HeLa cell lysates treated with a constant concentration of decorin revealed a progressive decrease of both secreted (Fig. 2, *E* and *F*) and cellular VEGFA (supplemental Fig. S2*C*) relative to mock (PBS) treated controls for up to 12 h. Down-regulation of secreted and cellular VEGFA was noted as early as 2 h (*cf.* Fig. 2*F* and supplemental Figs. S2*C*); thus, we conducted a *VEGFA* time course and found a gradual reduction of *VEGFA* mRNA persisting for up to 8 h in HeLa (supplemental Fig. S2*D*). Furthermore, immunofluorescent analysis confirmed reduction of cellular VEGFA in HeLa cells following decorin treatment (supplemental Fig. S2*E*).

Interestingly, cellular VEGFA levels maintained a stable decrease starting at 8 h and lasting for up to 24 h, which mirrored VEGFA expression. However, secreted VEGFA seemed to have a sharper decrease at later time points, potentially implicating an attenuation of the secretory pathway.

Collectively, our findings indicate that decorin affects VEGFA production in both transformed and normal cells and further corroborate the marked transcriptional inhibition obtained under normal oxygen tension. Moreover, these data postulate a firm role for decorin as a negative regulator of VEGFA by inhibiting its expression at multiple levels of control.

Decorin Suppresses VEGFA in the Presence of Constitutively-active HIF-1α under Normoxic Conditions—Further interrogation behind the mechanism of decorin-mediated suppression of VEGFA signaling led us to evaluate the role of HIF-1α based on the potent inhibition of *HIF1A* transcription under normoxic conditions (*cf.* Fig. 1). The *HIF1A* gene encodes a key basic helix-loop-helix transcription factor that dimerizes with the constitutively expressed HIF-1β/ARNT subunit to form a stable complex capable of recruiting transcriptional co-activators such as CBP/p300 to proximal promoters (97). Consequently, the genetic subsets targeted by HIF-1α are primarily responsible for orchestrating and executing the cellular hypoxic response that will drive angiogenesis. It is well established that

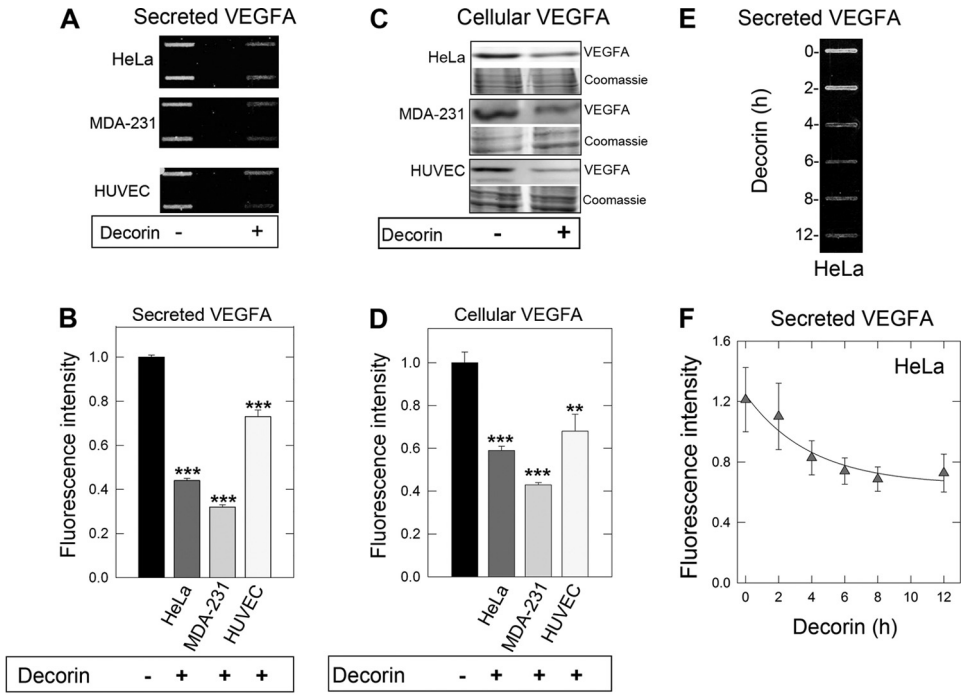

FIGURE 2. **Decorin potently attenuates VEGFA signaling.** *A*, slot blot analysis of tumor-conditioned medium in the absence or presence of 500 nM decorin following a 24-h incubation to evaluate effects on secreted VEGFA in cervical adenocarcinoma (HeLa), triple negative breast carcinoma (MDA-231), and normal human umbilical vein endothelial cells (HUVEC). *B*, quantification of secreted VEGFA signal intensity for the above described cell lines, normalized to total cell number. *C*, immunoblot analysis of HeLa, MDA-231, and HUVEC cell lysates treated in the presence or absence of decorin (500 nM) for 24 h. Lysates were recovered and separated by 10% SDS-PAGE and probed for cellular VEGFA. β-Actin served as an internal loading control. *D*, immunoblot quantification representing normalized fluorescence to β-actin for cellular VEGFA after decorin protein core treatment. *E*, slot blot analysis of HeLa tumor cell-conditioned medium treated with decorin protein core (500 nM) for the indicated time points. *F*, quantification of secreted VEGFA time course for the time intervals analyzed. Immunoassayed proteins via slot blot and Western blot were detected with IR-Dye-conjugated secondary antibodies amenable for visualization via the Odyssey Infrared Imaging System (LI-COR) with data representative of 2–3 independent experiments run in duplicate and reported as mean ± S.E. (**, $p < 0.01$; ***, $p < 0.001$).

VEGFA expression is transcriptionally driven by HIF-1α (89, 98).

Utilization of specific MDA-231(GFP$^+$) cell lines, which overexpress either wild-type HIF-1α (MDA-231 wtHIF-1α) or a mutated HIF-1α (MDA-231 mutHIF-1α) allowed for direct evaluation of HIF-1α function in normoxia. In the HIF-1α mutant, the proline residues residing within the oxygen-dependent degradation domain have been mutated to alanine (P402A and P564A) that culminate in a constitutively-active HIF-1α. This form is no longer a proper substrate for PHD2-mediated hydroxylation and subsequent protein Von Hippel-Lindau (pVHL)-dependent ubquitination leading to proteasomal degradation. Thus, activated HIF-1α is stable under normoxic conditions (78). We discovered that decorin evoked down-regulation of both wild-type and mutant HIF-1α (Fig. 3, *A* and *B*). Immunofluorescence detection of both HIF-1α and VEGFA showed a significant decrease in both wild-type and mutant cells (Fig. 3, *C* and *D*). We found that secreted VEGFA was also reduced in the two cell types (Fig. 3*E*), further supporting the data presented above. Thus, decorin evokes down-regulation of the HIF-1α protein in mammary carcinoma cells harboring either wild-type or a constitutively-active HIF-1α.

Consistent with this notion, pVHL, the E3-ubquitin ligase complex liable for degrading HIF-1α under normoxic conditions (99) was up-regulated nearly 2-fold in MDA-231 wtHIF-1α, but was unchanged in MDA-231 mutHIF-1α (supplemental Fig. S3*A*) following increasing concentrations of decorin. Further evaluation of pVHL in parental MDA-231 cells demonstrated a modest induction (supplemental Fig. S3*B*); however, this was in contrast to the nearly 40% inhibition of HIF-1α protein after 4 h (supplemental Fig. S3*B*), which is consistent with the above findings. Of note, treatment of HeLa demonstrated a similar trend of modestly induced pVHL correlating with reduced HIF-1α (not shown).

Collectively, these data posit a potential role of pVHL, in conjunction with the already declining *HIF1A* expression levels, for the early stages of HIF-1α antagonism. Therefore, inhibition of HIF-1α does not seem to rely as heavily on pVHL, instead decorin evokes a prominent transcriptional repression. This provides a novel role of attenuating traditional HIF-1α/VEGFA signaling under normoxic conditions to curb tumor growth.

Decorin Disables an Array of Activating Transcription Factors Essential for Proper Expression of HIF1A and VEGFA under Normoxia—To further investigate the potential mechanism of decorin anti-angiogenic activity, we performed a detailed expression analysis of pertinent transcription factors essential for driving the expression of both *HIF1A* and *VEGFA*. Multiple transcription factors are known to have consensus binding sites within the promoter of *VEGFA*, in particular numerous sites are present for Sp1 and AP-1 as well as a HIF-1α response element (89). Coincidentally, these factors are also essential for promoting and allowing *HIF1A* expression.

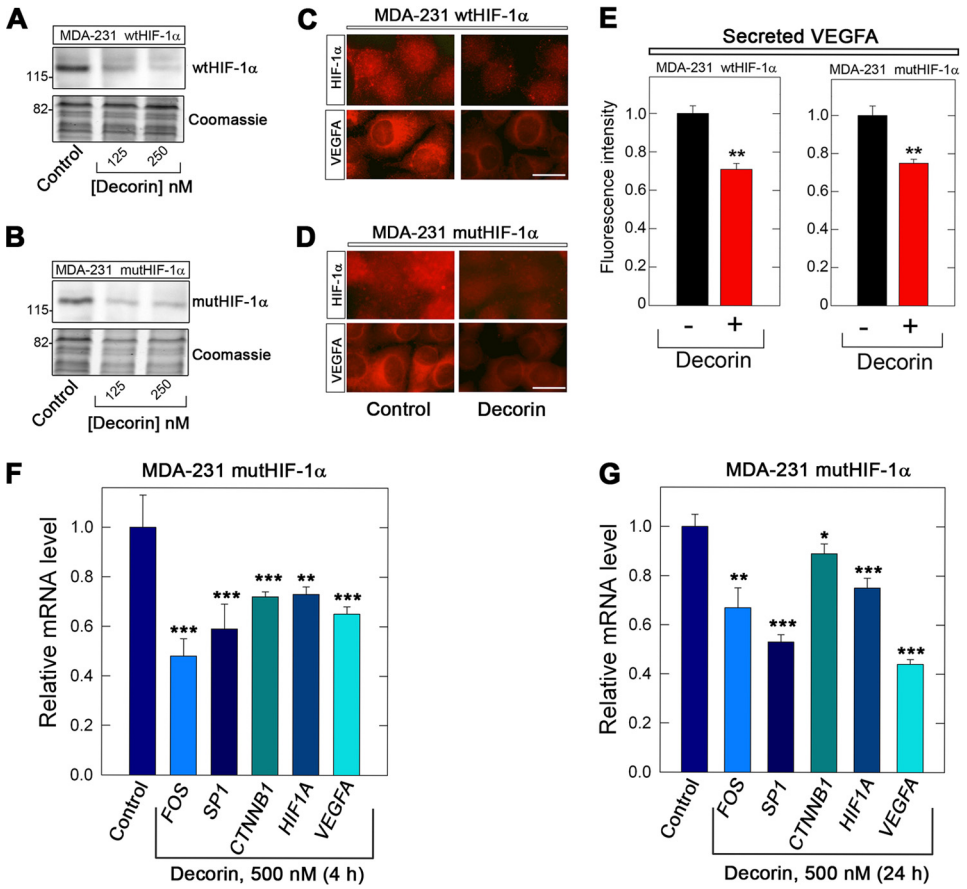

FIGURE 3. **Decorin suppresses HIF-1α and VEGFA in constitutively-activated HIF-1α MDA-231 cells under normoxic conditions and suppresses critical transcription factors needed for HIF1A and VEGFA expression.** *A* and *B*, immunoblot analysis of HIF-1α expression in either wild-type or mutant cell lines as indicated. Cells were exposed for 4 h to increasing concentrations of decorin. The *lower parts* of the blots were stained with Coomassie to demonstrate equal loading. The migration of molecular mass protein standards is shown on the *left*. *C* and *D*, immunolocalization of HIF-1α and VEGFA in either wild-type or mutant cell lines as indicated. The cells were treated for 4 h with decorin, fixed, permeabilized, and reacted with antibodies specific for either HIF-1α or VEGFA. *Bar* = 10 μm. *E*, quantification of secreted VEGFA obtained by slot blot analysis of media conditioned for 4 h by either wild-type or mutant cells as designated. *F* and *G*, gene expression analysis of critical pathway genes found to be essential for driving the expression of *HIF1A* and *VEGFA* after 4 h (*F*) or 24 h (*G*) of decorin as indicated. Data are representative of at least two independent trials run in quadruplicate and normalized to the endogenous housekeeping gene *ACTB*. Data are reported as percentage change ± S.E. as calculated according to the comparative $\Delta\Delta C_t$ method (*, $p < 0.05$; **, $p < 0.01$; ***, $p < 0.001$).

Taking this information into account we evaluated *FOS* and *SP1* expression within mutHIF-1α cells 4 and 24 h post-exposure to decorin. The expression of *FOS* was significantly decreased at both time points ($p < 0.001$ and 0.01, Fig. 3, *F* and *G*), with a greater reduction occurring after 4 h with some recovery after 24 h. A similar expression signature was obtained with *SP1* at both 4 and 24 h ($p < 0.001$, Fig. 3, *F* and *G*).

Next, *CTNNB1* (β-catenin) expression exhibited a reduction ($p < 0.001$, Fig. 3*F*) following 4 h; however, after 24 h, *CTNNB1* expression seemed to recover significantly (Fig. 3*G*), and return almost to baseline ($p < 0.05$, Fig. 3*G*). These data are congruent with the finding of seven TCF/LEF binding sites embedded within the proximal promoter of *VEGFA* (100) and thus enforce the critical role of β-catenin signaling in the promotion of VEGFA-mediated tumor angiogenesis. Furthermore, the expression of *HIF1A* decreased significantly at 4 h ($p < 0.01$, Fig. 3*F*) and this was protracted for up to 24 h ($p < 0.001$, Fig. 3*G*). Finally, in regard to *VEGFA* expression, both time points revealed a potent suppression in MDA-231 mutHIF-1α cells ($p < 0.001$, Fig. 3, *F* and *G*). Overall, these expression data corroborate the above mentioned protein and immunofluorescence data.

In summary, these data argue for a role of decorin in promoting a cessation of pro-angiogenic transcription via a potent reduction in multiple genes necessary for the expression of *HIF1A* and *VEGFA*. More importantly is the ability of decorin to achieve potent angiostasis in an activated HIF-1α cell line under normoxic conditions. Furthermore, classical Ras/MAPK signaling cascades emanating from RTKs such as Met (see below), are known to target and phosphorylate Sp1 via the p42/p44 MAPK, resulting in full activation and specific targeting of Sp1 to the proximal promoter of *VEGFA* for competent transactivation (101).

The Role of Met in Regulating Angiogenesis vis à vis VEGFA Signaling—We have previously shown that binding of decorin to Met is oppositional and subsequent receptor internalization and degradation ensues (52). Therefore, focusing on the prevalent association of Met in the process of tumor angiogenesis and the documented interaction with decorin, we determined the link of Met in the process of decorin-mediated angiostasis. This link was established via the transfection of a mixture of three validated siRNAs targeting Met mRNA. We reasoned that Met down-regulation at the mRNA level would mimic the proteasomal-induced degradation of Met evoked by exogenous decorin.

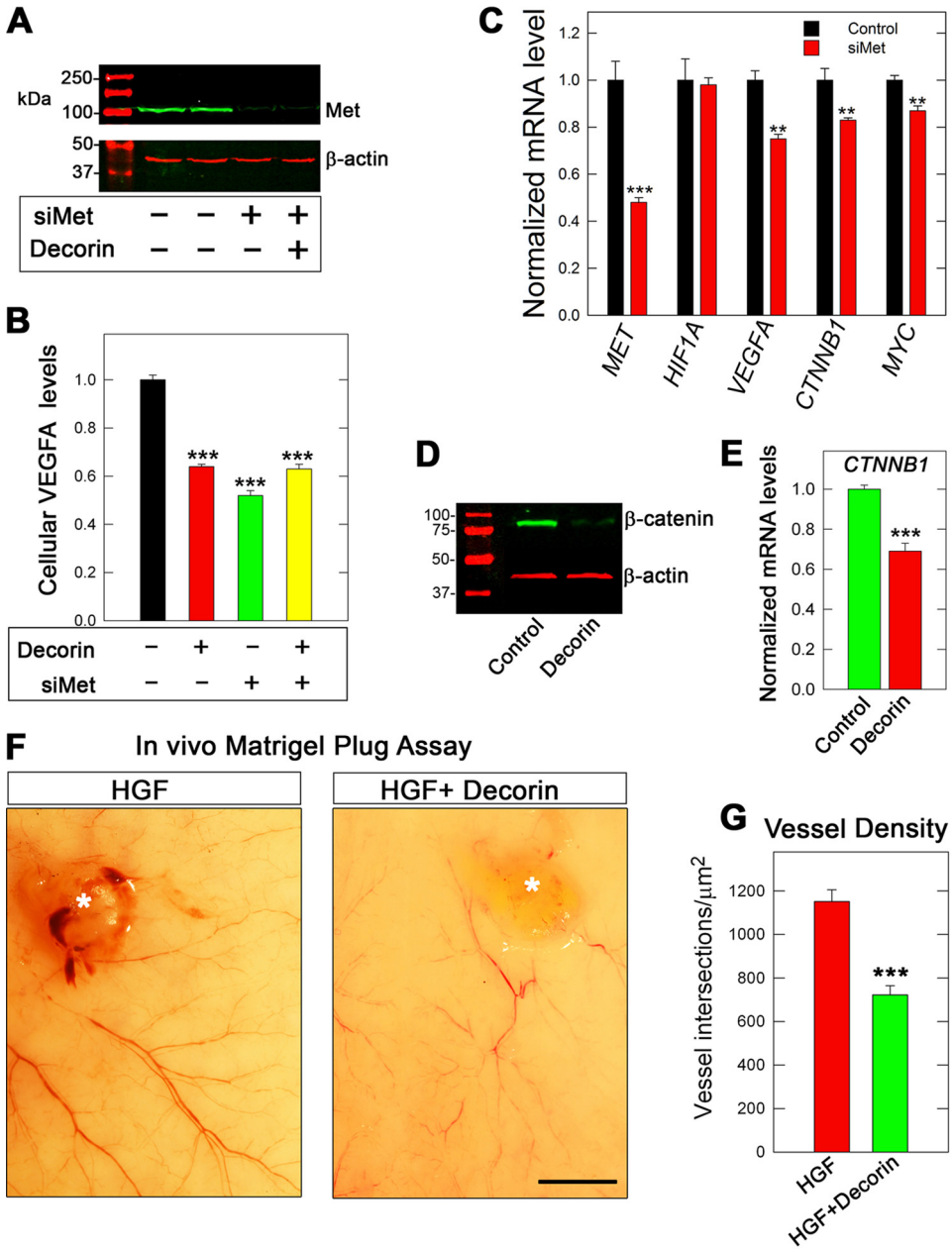

FIGURE 4. **Decorin-mediated attenuation of HGF/Met signaling evokes potent angiostasis.** *A,* immunoblot verification of Met protein depletion following transient transfection of cognate targeting siRNA (80 pM) (designated as siMet) in HeLa 48 h post-transfection. *B*, immunoblot analysis following positive verification of Met knockdown HeLa lysates probed for cellular VEGFA under conditions of control, decorin (24 h, 500 nM), siMet (80 pM), or combined treatment and appear as a quantification of cellular VEGFA fluorescent intensity after normalizing to β-actin. *C,* expression data gained from qPCR analysis of pertinent genes in the presence of siMet (80 pM). Verification of siRNA functionality is delineated in this graph for Met. *D*, HeLa lysates were immunoblotted for β-catenin and β-actin (as a loading control) under the influence of decorin (500 nM) for 24 h. *E*, HeLa cDNA libraries evaluated for *CTNNB1* via qPCR under the same experimental conditions as in *D*. *F,* micrographs depicting high resolution digital images of mouse dorsal skin as it appears from the interior, 14 days after subcutaneous injection with either Matrigel (80 ml combined with ~10^6 MDA-231 GFP^+ cells) and HGF (10 ng/ml) in the absence (*F, left panel*) or presence (*F, right panel*) of decorin proteoglycan (200 nM). *Asterisk* denotes Matrigel plug and tumor location. *G*, morphometric analysis of blood vessel density reported as vessel intersections per μm^2. Density was calculated by determining the average number of times the newly formed angiogenic vessels intersected a grid, representing a standard area of 1 mm^2, which were superimposed onto the images. The values represent the mean ± S.E. ($n = 600$). *Bar* = 4 mm. Immunoblot and Met knockdown experiments represent an average of at least two independent experiments performed in duplicate with quantification representing the average ± S.E. for cellular VEGFA. Gene expression data are representative of 2–3 independent trials reported as fold-change ± S.E. (*, $p < 0.05$; **, $p < 0.01$; ***, $p < 0.001$).

The siRNA targeting Met reduced the receptor to barely detectable levels without affecting β-actin levels (Fig. 4*A*). Importantly, knockdown of Met recapitulated the down-regulation of cellular VEGFA (Fig. 4*B*). Furthermore, dual treatment of HeLa cells with both targeting siRNA followed by a 24-h incubation with decorin did not result in additional inhibition of cellular VEGFA, in agreement with Met acting as the main signaling receptor for decorin-evoked inhibition of VEGFA (Fig. 4*B*).

As discussed above, decorin suppresses the transcription of targets critical for the promotion of angiogenesis. Therefore, to dissect if decorin is transducing these anti-angiogenic effects

via Met, we used siRNA targeting Met. This strategy achieved Met transcript reduction by ~50% (Fig. 4*C*), relative to the scrambled siRNA control. Interestingly, depletion of Met alone induced transcriptional changes in *VEGFA* and *CTNNB1* analogous to decorin-treated HeLa cells (Fig. 4, *C* and *E*), but to a lesser degree. Finally, *MYC* a downstream target of the Met/β-catenin antagonism (52), was found to change only modestly (Fig. 4*C*).

Surprisingly, *HIF1A* expression was not appreciably affected under these conditions (Fig. 4*C*). Several reasons could account for this discrepancy such as the requirement of decorin to evoke changes in *HIF1A* expression, *vis à vis* Met engagement, compensatory mechanisms mediated via HIF-2α, or because signaling is being integrated by decorin over multiple RTKs, such as the EGFR.

As a primary downstream effector of Met (52), β-catenin was prominently reduced via decorin (Fig. 4*D*). This inhibition also extended to *CTNNB1* transcripts (Fig. 4*E*), to an extent comparable with MDA-231 wtHIF-1α as shown previously (*cf.* Fig. 3*F*). As decorin down-regulates Met protein levels via cavaeolar-mediated endocytosis and proteasomal-dependent degradation (47), we tested the effects of decorin on *MET* transcript levels. Notably, we found a significant reduction in the expression of *MET* (*cf.* Fig. 1*B*) indicating disruption of a positive feedback loop that exists between Met and β-catenin upon decorin engagement (102). It is tempting to speculate that decorin is abrogating both β-catenin and Sp1 signaling subsequent to Met degradation, resulting in transcriptional inhibition of the *VEGFA* locus. Importantly, this fosters a scenario wherein a growth factor receptor-dependent mechanism of HIF-1α regulation is feasible, and is congruent with the biological activity decorin exerts on Met (103). Notably, decorin-null mice have increased expression of β-catenin in the enteric epithelium (57).

Further proof of principle of decorin-mediated angiostasis was established by employing a tumor xenograft mouse Matrigel assay. To this end, we injected ~10^6 MDA-231 (GFP^+) cells mixed with ~80 μl of Matrigel and 10 ng/ml of HGF in the absence or presence of decorin (200 nM) into four dorsal subcutaneous regions of severe combined immunodeficient mice. After 14 days with HGF, a strong angiogenic reaction was achieved surrounding the tumors (*asterisk*, Fig. 4*F, left panel*). This is in stark contrast to the combined treatment of decorin and HGF for the same time period (Fig. 4*F, right panel, asterisk*). Morphometric analysis of the vessel density revealed a marked suppression of vascularity associated with the decorin-containing xenografts ($p < 0.001$, Fig. 4*G*).

These *in vivo* findings argue a very strong case for the ability of decorin to retard tumor angiogenesis in MDA-231 tumor xenograft Matrigel assays. These data establish and enforce a role of Met as being involved in a noncanonical Wnt/β-catenin signaling pathway induced by HGF to promote tumor angiogenesis, *vis à vis* VEGFA, which can be abrogated by decorin.

Decorin Inhibits Induction and Activity of Matrix Metalloproteinases—Aggressive neoplasms often show increased expression of a class of zinc-dependent gelatinases known as MMPs capable of degrading the matrix as well as liberating a host of pro-angiogenic factors (104, 105). Primarily pertinent for the current study is the ability of matrix-bound VEGFA to be released, making the factor readily available for use by the surrounding angiogenic cells (106). Taking this into account, we analyzed the expression and activity of MMP-9 and MMP-2, both of which are under the control of β-catenin signaling (107). MMPs are secreted by the host cell as a zymogen (otherwise known as the "proform"), followed by a proteolytic cleavage event to yield the catalytically active enzyme. Thus, to assess the activity of secreted MMPs, media conditioned for 24 h by HeLa cells in the absence or presence of exogenous decorin (500 nM) were subjected to gelatin zymography. This functional assay revealed a dramatic reduction in the activity of MMP-9 as well as a more modest, but still significant, decrease in the activity of MMP-2 (Fig. 5*A*) relative to control conditioned medium ($p < 0.001$ and $p < 0.05$, respectively, Fig. 5*B*). In agreement with gel zymography, utilization of a MMP-9 fluorescence resonance energy transfer (FRET) probe assay revealed >50% reduction in the activity of endogenous MMP-9 present in HeLa-conditioned medium following decorin treatment (Fig. 5*C*). In support of these functional data, gene expression analysis revealed an effective decrease in *MMP9* ($p < 0.001$, Fig. 5*D*) and a modest but statistically significant reduction in *MMP2* ($p < 0.05$, Fig. 5*D*). We then performed ELISA with antibodies specific for both MMPs and showed a significant decrease in secreted MMP-9 ($p < 0.001$, Fig. 5*E*) without any significant reduction in secreted MMP-2 (Fig. 5*F*). These data are uniformly consistent with the gelatin zymography and gene expression data presented above.

Next, we evaluated the role of a membrane-type MMP, known as MT1-MMP (or MMP-14), which is pro-angiogenic and pro-invasive via the cleavage and activation of MMP-2 and MMP-9 (108, 109). To this end, we carried out immunoblotting to detect MT1-MMP in our HeLa samples and subsequently found no significant change in MT1-MMP levels (Fig. 5*G*). We also found no appreciable changes in the expression of *MMP14* (not shown).

Collectively, these data indicate that decorin is most likely not attenuating MMP-2/9 activity or expression via modulation of a presumed upstream activator, *i.e.* MT1-MMP. Moreover, these data provide further evidence for the potent transcriptional control decorin exerts over these loci by abrogating noncanonical β-catenin signaling.

Finally we evaluated the role of TIMP3, a secreted protein that binds tightly to the extracellular matrix and is also a direct inhibitor of ADAM-17/TACE (110). TIMP3 has also been proposed to be a tumor suppressor in several human cancers such as kidney, colon, brain, memingomas, and non-small cell lung cancers (111–113). Interestingly, TIMP3 has also been reported to reduce Met receptor shedding (114). According to the array (*cf.* Fig. 1), decorin induces TIMP3 expression; thus, we evaluated HeLa cell-conditioned medium and found an almost 5-fold increase in secreted TIMP3 (supplemental Fig. S4*A*). Furthermore, immunofluorescent analysis of MDA-231(GFP^+) tumor xenograft cyrosections also revealed an abundant increase in TIMP3 signal intensity (supplemental Fig. S4*B*), thus indicating a decorin-dependent induction of TIMP3 *in vitro* and *in vivo*.

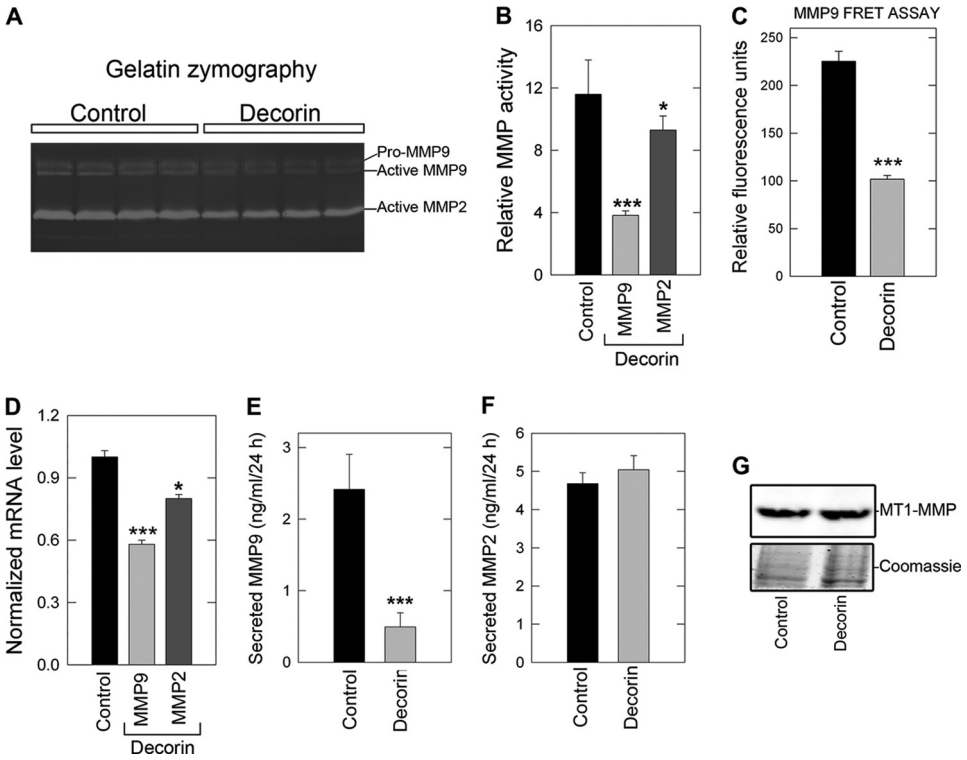

FIGURE 5. **Decorin prevents the expression and activation of matrix metalloproteases necessary for tumor extravasation, metastasis, and VEGFA liberation.** *A*, HeLa cell-conditioned medium treated with PBS or decorin (500 nM) for 24 h was evaluated for enzymatic activity of MMP-2 and MMP-9 via gelatin zymography. *B*, quantification of MMP-9 and MMP-2 enzymatic activity as determined in *A* as a function of relative MMP activity. *C*, HeLa interrogated 24 h post-decorin (500 nM) addition for the expression of *MMP9* and *MMP2* transcripts via qPCR. *D*, ELISA of total MMP-9 and MMP-2 as indicated and found in HeLa cell-conditioned medium (ng/ml/24 h) in the presence or absence of decorin (500 nM). Gene expression changes are reported as the average fold-change ± S.E. collated over 2–3 trials performed in quadruplicate and normalized to the housekeeping gene *ACTB*. Gel zymography and total MMP-2/9 ELISA were repeated twice in triplicate (*, $p < 0.05$; ***, $p < 0.001$).

We conclude that decorin suppresses the expression and functional activity of MMP-2/9 at least in part by antagonizing Met signaling. This would result in a protracted degradation and inhibition of β-catenin in a non-canonical Wnt, RTK-dependent manner insofar as both MMP-2 and MMP-9 are direct transcriptional targets of β-catenin (107).

Decorin Induces Thrombospondin-1 Both in Cell Cultures and Tumor Xenografts—Next, we determined the levels of secreted thrombospondin-1 in medium conditioned by HeLa cells that were exposed to either vehicle (control) or decorin (500 nM) for 24 h. Using quantitative dot blot analysis, we found a marked increase in the secretion of thrombospondin-1 (Fig. 6*A*), whereas the secretion of perlecan (internal control) was not appreciably changed (Fig. 6*B*). Similarly, the cellular levels of thrombospondin-1 were also significantly increased by decorin (Fig. 6*C*).

Next, we utilized mice bearing HeLa tumor xenografts that were treated with intraperitoneal injections of decorin (5 mg/kg) every other day over a period of 23 days. At the end of the treatment, the volume of the decorin-treated tumors was approximately half the size of vehicle-treated counterparts ($p < 0.001$, $n = 6$ per group, Fig. 6*D*). Immunofluorescence analysis of frozen tumor sections showed a marked induction of endogenous human thrombospondin-1 in the treated tumor xenografts (Fig. 6*E*). Concurrently, the amount of endogenous VEGFA was markedly reduced in the decorin-treated xenografts (supplemental Fig. S5).

Further *in vivo* relevance of decorin-mediated angiostasis was determined via qPCR to evaluate the expression of pro-angiogenic markers present in the tumor xenografts. In the treated xenografts, there was a substantial down-regulation of *MMP2*, *MMP9*, and *VEGFA* ($p < 0.001$, Fig. 6*F*) and a marked up-regulation (up to 15-fold) of *THBS1* ($p < 0.001$, Fig. 6*G*) transcription. Overall, these data correlate well with the *in vitro* findings and further strengthen the concept and current rationale while providing a proof-of-principle for decorin-mediated inhibition of VEGFA-mediated tumor angiogenesis.

Systemic Administration of Decorin Inhibits Pro-angiogenic Markers in Orthotopic Tumor Xenografts—To further strengthen the *in vivo* relevance of our data, we generated orthotopic mammary tumor xenografts using triple-negative breast carcinoma cells MDA-231(GFP^+). In this case, systemic treatment with the decorin protein core resulted in a marked induction of endogenous human thrombospondin-1 by systemic delivery of decorin (supplemental Fig. S6*A*). In addition, the HeLa xenografts demonstrated an almost complete loss of cellular VEGFA within the decorin-treated cohort relative to control animals when analyzed via immunofluorescence and quantified as three-dimensional surface plots of the fluorescent signal (supplemental Fig. S6*B*). Collectively, our results indicate that decorin can simultaneously down-regulate pro-angiogenic factors and up-regulate anti-angiogenic factors in two animal models of tumorigenesis.

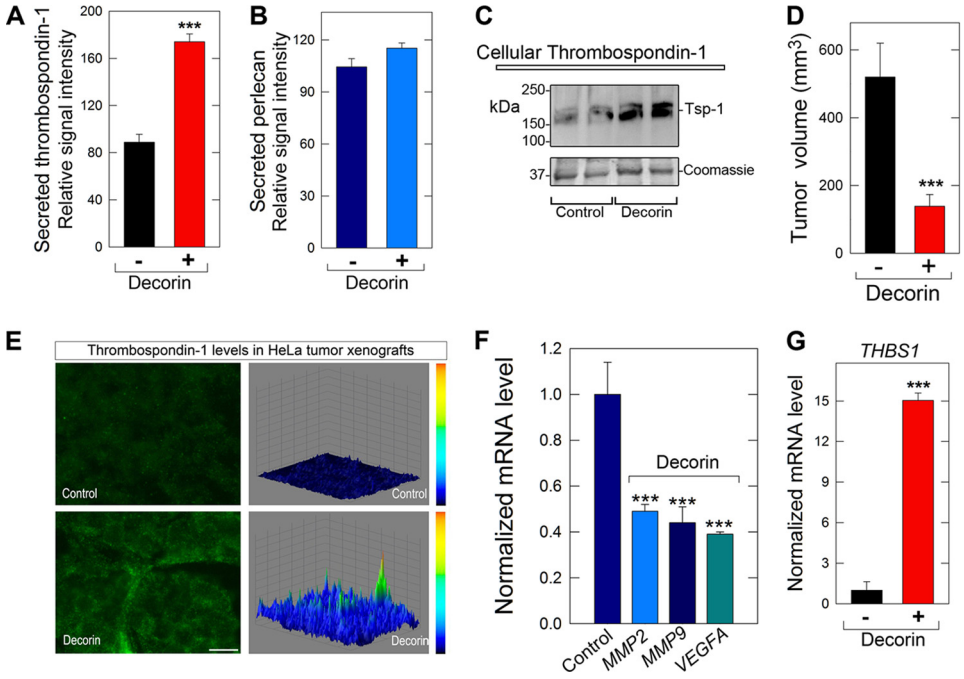

FIGURE 6. **Decorin induces the anti-angiogenic factor thrombospondin-1 both in cell cultures and in tumor xenografts.** *A* and *B*, media conditioned by HeLa exposed to either vehicle (control) or decorin (500 nM) for 24 h were evaluated for the presence of secreted thrombospondin-1 and perlecan (as control). Notice that the levels of thrombospondin-1 are significantly elevated by exogenous decorin (***, $p < 0.001$, $n = 4$). The values were obtained by utilizing dot blots with serial dilutions of conditioned media (400–12.5 μl) and anti-thrombospondin-1 or anti-perlecan antibodies and reported as the relative signal intensities of either secreted thrombospondin-1 or perlecan, respectively. *C*, Western blot of cellular thrombospondin-1 from HeLa cells treated with or without decorin as indicated. *D*, tumor volume of HeLa xenografts at day 23. Mice bearing HeLa xenografts were treated with intraperitoneal injections of decorin (5 mg/kg) every other day over a period of 23 days (***, $p < 0.001$, $n = 6$ per group). *E*, induction of thrombospondin-1 in the tumor xenografts by systemic delivery of decorin. The images show representative frozen sections of HeLa xenografts at day 23 post-decorin treatment or control immunostained for thrombospondin-1. All micrographs were imaged using the same exposure and gain. The *right panels* are three-dimensional surface plots of the corresponding images to the *left*, which were generated with ImageJ software as described before (47). *Bar* = ~10 μm. *F* and *G*, qPCR analysis of mRNA extracted from HeLa xenografts at day 23 post-decorin or control treatment. Data are from three independent trials run in quadruplicate and normalized to the endogenous housekeeping gene *ACTB*. (***, $p < 0.001$).

DISCUSSION

The steps involved in tumor progression have been derived from multiple animal models and reflect discrete changes within the genome via activation of oncogenes or the silencing of tumor suppressor genes that drive a normal cell through transformation to a malignant phenotype (115). A key milestone on the path to cancer progression is the development of a competent tumor vasculature to provide a blood supply as well as a conduit for metastasis. This event is mediated via a discrete step known as the angiogenic switch, which results in an imbalance of key pro-angiogenic cytokines and angiogenic inhibitors. Previous reports implicate decorin as a powerful inhibitor of tumor angiogenesis (73). In our current working model (Fig. 7) stromal decorin engages and abrogates the HGF/Met signaling axis, acting as a potent suppressor of VEGFA-mediated tumor angiogenesis. Decorin binding to Met initiates receptor internalization via increased phosphorylation of Tyr^{1003}, which is a recruitment site for the E3 ubquitin ligase c-Cbl. This mechanism triggers caveolar-mediated endocytosis of the receptor complex, culminating in the transcriptional repression of HIF-1α, β-catenin, MYC, and SP1 under normoxic conditions, coincident with decreased protein levels and proteasomal degradation of HIF-1α, β-catenin, and MYC (Fig. 7). The combinatorial effect of inhibiting this constellation of transcription factors results in the impairment of *VEGFA*, *MMP2*, and *MMP9* expression, and a simultaneous transcriptional induction of *THBS1* and *TIMP3*, potent inhibitors of angiogenesis and the MMP family. Moreover, we envisage that a concurrent reduction of MMP-2/9 activity coupled with induction of thrombospondin-1 and TIMP3 allows for potent angiostasis in the matrix, acting to further restrict matrix-bound VEGFA from engaging cognate receptors (*e.g.* VEGF-R2) on the surface of tumor endothelial cells (Fig. 7). The potential involvement of MT1-MMP (MMP-14) was evaluated and found to be unchanged because this membrane-type MMP is postulated to orchestrate several steps directly during cancer progression including the degradation of physical barriers (*e.g.* laminin-5) necessary for cancer cell invasion (invadopodia), migration, activation of TGF-β, and indirectly for tumor angiogenesis through cleavage and activation of pro-angiogenic MMP-2 and MMP-9, at the cell surface. MT1-MMP has also been reported to remodel the basement membrane and regulate cell proliferation during renal development (116).

Notably, thrombospondin-1 expression is negatively regulated by Myc (117, 118), thereby allowing establishment of the angiogenic switch and tumor progression, particularly of mammary epithelial cells (119). Thus, an additional way that decorin could induce thrombospondin-1 would be via repression of Myc (52). Moreover, HGF induces a severe repression of *THBS1* expression via activation of Met (77). Thus, interference of the HGF/Met signaling axis, as coordinated by decorin, not only serves to repress VEGFA but also acts to potently induce

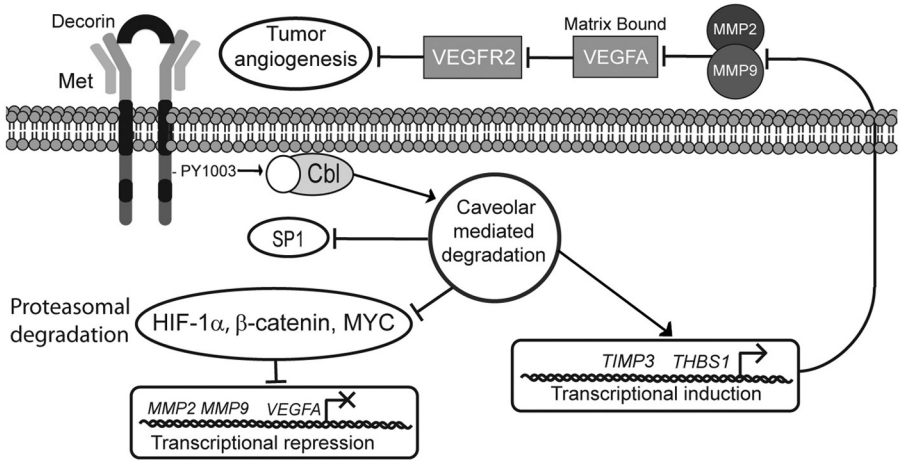

FIGURE 7. **Schematic representation of proposed model for decorin-evoked angiostatic activity.** Please refer to the text for a detailed explanation.

thrombospondin-1, further preventing Met- and VEGFA-mediated tumor angiogenesis.

We previously reported that stable expression of decorin in several malignant cell lines led to inhibition of endogenous VEGFA expression (73). However, the mechanism of this effect was not investigated. In the present study we have expanded these original observations and unmasked a mechanism that is controlled by a decorin-evoked down-regulation of Met, and perhaps other RTKs. An additional novelty of this current study lies in the identification of a normoxic and HIF-1α-dependent mechanism as a molecular basis for these findings. Furthermore, at the time of publication of our previous study, we were unaware of the recently established high affinity interaction of decorin with the pro-angiogenic Met receptor (51). Abrogating the EGFR activity by functionally blocking the receptor with mAb425 or utilizing AG1478, in the presence of decorin, was able to evoke rapid activation of Met followed by internalization and down-regulation of total Met levels, implicating Met as the primary receptor for decorin. Finally, it was subsequently found that Met has a substantially higher affinity for decorin relative to that of EGFR (51).

This angiostatic effect has probable implications that attenuate the initial stages of tumor angiogenesis. In this phase, which precedes the activation of the angiogenic switch, tumor hypoxia has not yet reached a biologically relevant threshold to induce tumor vascularization. This delineates a compelling role for matrix-derived residents as being essential modulators of early angiogenic events.

Our data presented here seemingly contradicts a previously published study (120), which reported that decorin is able to induce VEGF production by recruiting Sp1, HIF-1α, and STAT3 to the cognizant response elements within the promoter of *VEGF*. This study, however, was performed with murine cerebral endothelial cells (120). Our study, in contrast, was conducted in two human carcinoma cell lines. In this context, the molecular repertoire and genomic profile of malignant human cervical and breast cell lines compared with normal mouse cerebral endothelial cells make comparison difficult. Furthermore, our data concerning the effect of decorin for normal human endothelial cells suggest an inhibitory role, which is supported by a recent study demonstrating decorin antagonizes VEGFR2 in human extravillous trophoblasts and interfering with migration by attenuating ERK1/2 signaling (121).

In conclusion, our data demonstrate a novel antagonistic interaction of the HGF-Met signaling axis leading to a marked and sustainable inhibition of VEGFA-mediated angiogenesis under normoxic conditions. Potential therapeutic induction of this mechanism of decorin, acting as a potent angiostatic agent, will attenuate critical steps in the progression of a malignant neoplasm and will have broad medicinal applications as an angiostatic modality.

Acknowledgment—We thank Nutan Pal for help in the initial stages of this project.

REFERENCES

1. Bissell, M. J., and Hines, W. C. (2011) *Nat. Med.* **17,** 320–329
2. Ferrara, N., and Kerbel, R. S. (2005) Angiogenesis as a therapeutic target. *Nature* **438,** 967–974
3. Iozzo, R. V. (1998) Matrix proteoglycans. From molecular design to cellular function. *Annu. Rev. Biochem.* **67,** 609–652
4. Iozzo, R. V. (2005) Basement membrane proteoglycans. From cellar to ceiling. *Nat. Rev. Mol. Cell. Biol.* **6,** 646–656
5. Iozzo, R. V., and Sanderson, R. D. (2011) Proteoglycans in cancer biology, tumor microenvironment, and angiogenesis. *J. Cell. Mol. Med.* **15,** 1013–1031
6. Iozzo, R. V., and Murdoch, A. D. (1996) Proteoglycans of the extracellular environment. Clues from the gene and protein side offer novel perspectives in molecular diversity and function. *FASEB J.* **10,** 598–614
7. Iozzo, R. V. (1999) The biology of the small leucine-rich proteoglycans. Functional network of interactive proteins. *J. Biol. Chem.* **274,** 18843–18846
8. Schaefer, L., and Iozzo, R. V. (2008) Biological functions of the small leucine-rich proteoglycans. From genetics to signal transduction. *J. Biol. Chem.* **283,** 21305–21309
9. Danielson, K. G., Baribault, H., Holmes, D. F., Graham, H., Kadler, K. E., and Iozzo, R. V. (1997) Targeted disruption of decorin leads to abnormal collagen fibril morphology and skin fragility. *J. Cell Biol.* **136,** 729–743
10. Reed, C. C., and Iozzo, R. V. (2002) The role of decorin in collagen fibrillogenesis and skin homeostasis. *Glycoconj. J.* **19,** 249–255
11. Keene, D. R., San Antonio, J. D., Mayne, R., McQuillan, D. J., Sarris, G., Santoro, S. A., and Iozzo, R. V. (2000) Decorin binds near the C terminus of type I collagen. *J. Biol. Chem.* **275,** 21801–21804
12. Zhang, G., Ezura, Y., Chervoneva, I., Robinson, P. S., Beason, D. P., Carine, E. T., Soslowsky, L. J., Iozzo, R. V., and Birk, D. E. (2006) Decorin regulates assembly of collagen fibrils and acquisition of biomechanical

properties during tendon development. *J. Cell. Biochem.* **98,** 1436–1449
13. Zhang, G., Chen, S., Goldoni, S., Calder, B. W., Simpson, H. C., Owens, R. T., McQuillan, D. J., Young, M. F., Iozzo, R. V., and Birk, D. E. (2009) Genetic evidence for the coordinated regulation of collagen fibrillogenesis in the cornea by decorin and biglycan. *J. Biol. Chem.* **284,** 8888–8897
14. Rühland, C., Schönherr, E., Robenek, H., Hansen, U., Iozzo, R. V., Bruckner, P., and Seidler, D. G. (2007) The glycosaminoglycan chain of decorin plays an important role in collagen fibril formation at the early stages of fibrillogenesis. *FEBS J.* **274,** 4246–4255
15. Sanches, J. C., Jones, C. J., Aplin, J. D., Iozzo, R. V., Zorn, T. M., and Oliveira, S. F. (2010) Collagen fibril organization in the pregnant endometrium of decorin-deficient mice. *J. Anat.* **216,** 144–155
16. Kalamajski, S., and Oldberg, A. (2010) The role of small leucine-rich proteoglycans in collagen fibrillogenesis. *Matrix Biol.* **29,** 248–253
17. Robinson, P. S., Lin, T. W., Jawad, A. F., Iozzo, R. V., and Soslowsky, L. J. (2004) Investigating tendon fascicle structure-function relationships in a transgenic-age mouse model using multiple regression models. *Ann. Biomed. Eng.* **32,** 924–931
18. Robinson, P. S., Huang, T. F., Kazam, E., Iozzo, R. V., Birk, D. E., and Soslowsky, L. J. (2005) Influence of decorin and biglycan on mechanical properties of multiple tendons in knockout mice. *J. Biomech. Eng.* **127,** 181–185
19. Fust, A., LeBellego, F., Iozzo, R. V., Roughley, P. J., and Ludwig, M. S. (2005) Alterations in lung mechanics in decorin-deficient mice. *Am. J. Physiol. Lung Cell Mol. Physiol.* **288,** L159-L166
20. Ferdous, Z., Wei, V. M., Iozzo, R., Höök, M., and Grande-Allen, K. J. (2007) Decorin-transforming growth factor- interaction regulates matrix organization and mechanical characteristics of three-dimensional collagen matrices. *J. Biol. Chem.* **282,** 35887–35898
21. Elliott, D. M., Robinson, P. S., Gimbel, J. A., Sarver, J. J., Abboud, J. A., Iozzo, R. V., and Soslowsky, L. J. (2003) Effect of altered matrix proteins on quasilinear viscoelastic properties in transgenic mouse tail tendons. *Ann. Biomed. Eng.* **31,** 599–605
22. Järveläinen, H., Puolakkainen, P., Pakkanen, S., Brown, E. L., Höök, M., Iozzo, R. V., Sage, H., and Wight, T. N. (2006) *Wound Rep. Regen.* **14,** 443–452
23. Baghy, K., Dezso, K., László, V., Fullár, A., Péterfia, B., Paku, S., Nagy, P., Schaff, Z., Iozzo, R. V., and Kovalszky, I. (2011) Ablation of the decorin gene enhances experimental hepatic fibrosis and impairs hepatic healing in mice. *Lab. Invest.* **91,** 439–451
24. Brown, E. L., Wooten, R. M., Johnson, B. J., Iozzo, R. V., Smith, A., Dolan, M. C., Guo, B. P., Weis, J. J., and Höök, M. (2001) Resistance to Lyme disease in decorin-deficient mice. *J. Clin. Invest.* **107,** 845–852
25. Liang, F. T., Brown, E. L., Wang, T., Iozzo, R. V., and Fikrig, E. (2004) Protective niche for *Borrelia burgdorferi* to evade humoral immunity. *Am. J. Pathol.* **165,** 977–985
26. Goldberg, M., Septier, D., Rapoport, O., Iozzo, R. V., Young, M. F., and Ameye, L. G. (2005) Targeted disruption of two small leucine-rich proteoglycans, biglycan and decorin, excerpts divergent effects on enamel and dentin formation. *Calcif. Tissue Int.* **77,** 297–310
27. Haruyama, N., Sreenath, T. L., Suzuki, S., Yao, X., Wang, Z., Wang, Y., Honeycutt, C., Iozzo, R. V., Young, M. F., and Kulkarni, A. B. (2009) Genetic evidence for key roles of decorin and biglycan in dentin mineralization. *Matrix Biol.* **28,** 129–136
28. Corsi, A., Xu, T., Chen, X. D., Boyde, A., Liang, J., Mankani, M., Sommer, B., Iozzo, R. V., Eichstetter, I., Robey, P. G., Bianco, P., and Young, M. F. (2002) Phenotypic effects of biglycan deficiency are linked to collagen fibril abnormalities, are synergized by decorin deficiency, and mimic Ehlers-Danlos-like changes in bone and other connective tissues. *J. Bone Miner. Res.* **17,** 1180–1189
29. Brandan, E., Cabello-Verrugio, C., and Vial, C. (2008) Novel regulatory mechanisms for the proteoglycans decorin and biglycan during muscle formation and muscular dystrophy. *Matrix Biol.* **27,** 700–708
30. Zoeller, J. J., Pimtong, W., Corby, H., Goldoni, S., Iozzo, A. E., Owens, R. T., Ho, S. Y., and Iozzo, R. V. (2009) A central role for decorin during vertebrate convergent extension. *J. Biol. Chem.* **284,** 11728–11737
31. Bi, Y., Stuelten, C. H., Kilts, T., Wadhwa, S., Iozzo, R. V., Robey, P. G., Chen, X. D., and Young, M. F. (2005) Extracellular matrix proteoglycans control the fate of bone marrow stromal cells. *J. Biol. Chem.* **280,** 30481–30489
32. Weis, S. M., Zimmerman, S. D., Shah, M., Covell, J. W., Omens, J. H., Ross, J., Jr., Dalton, N., Jones, Y., Reed, C. C., Iozzo, R. V., and McCulloch, A. D. (2005) A role for decorin in the remodeling of myocardial infarction. *Matrix Biol.* **24,** 313–324
33. Chen, S., Sun, M., Meng, X., Iozzo, R. V., Kao, W. W., and Birk, D. E. (2011) Pathophysiological mechanisms of autosomal dominant congenital stromal corneal dystrophy. C-terminal-truncated decorin results in abnormal matrix assembly and altered expression of small leucine-rich proteoglycans. *Am. J. Pathol.* **179,** 2409–2419
34. Schaefer, L., Macakova, K., Raslik, I., Micegova, M., Gröne, H. J., Schönherr, E., Robenek, H., Echtermeyer, F. G., Grässel, S., Bruckner, P., Schaefer, R. M., Iozzo, R. V., and Kresse, H. (2002) Absence of decorin adversely influences tubulointerstitial fibrosis of the obstructed kidney by enhanced apoptosis and increased inflammatory reaction. *Am. J. Pathol.* **160,** 1181–1191
35. Schaefer, L., Mihalik, D., Babelova, A., Krzyzankova, M., Gröne, H. J., Iozzo, R. V., Young, M. F., Seidler, D. G., Lin, G., Reinhardt, D. P., and Schaefer, R. M. (2004) Regulation of fibrillin-1 by biglycan and decorin is important for tissue preservation in the kidney during pressure-induced injury. *Am. J. Pathol.* **165,** 383–396
36. Schaefer, L., Tsalastra, W., Babelova, A., Baliova, M., Minnerup, J., Sorokin, L., Gröne, H. J., Reinhardt, D. P., Pfeilschifter, J., Iozzo, R. V., and Schaefer, R. M. (2007) Decorin-mediated regulation of fibrillin-1 in the kidney involves the insulin-like growth factor-I receptor and mammalian target of rapamycin. *Am. J. Pathol.* **170,** 301–315
37. Williams, K. J., Qiu, G., Usui, H. K., Dunn, S. R., McCue, P., Bottinger, E., Iozzo, R. V., and Sharma, K. (2007) Decorin deficiency enhances progressive nephropathy in diabetic mice. *Am. J. Pathol.* **171,** 1441–1450
38. Schaefer, L. (2011) Small leucine-rich proteoglycans in kidney disease. *J. Am. Soc. Nephrol.* **22,** 1200–1207
39. Merline, R., Moreth, K., Beckmann, J., Nastase, M. V., Zeng-Brouwers, J., Tralhão, J. G., Lemarchand, P., Pfeilschifter, J., Schaefer, R. M., Iozzo, R. V., and Schaefer, L. (2011) Signaling by the matrix proteoglycan decorin controls inflammation and cancer through PDCD4 and MicroRNA-21. *Sci. Signal.* **4,** ra75
40. Iozzo, R. V., Bolender, R. P., and Wight, T. N. (1982) Proteoglycan changes in the intercellular matrix of human colon carcinoma. An integrated biochemical and stereologic analysis. *Lab. Invest.* **47,** 124–138
41. Adany, R., Heimer, R., Caterson, B., Sorrell, J. M., and Iozzo, R. V. (1990) Altered expression of chondroitin sulfate proteoglycan in the stroma of human colon carcinoma. Hypomethylation of PG-40 gene correlates with increased PG-40 content and mRNA levels. *J. Biol. Chem.* **265,** 11389–11396
42. Iozzo, R. V., Moscatello, D. K., McQuillan, D. J., and Eichstetter, I. (1999) Decorin is a biological ligand for the epidermal growth factor receptor. *J. Biol. Chem.* **274,** 4489–4492
43. Moscatello, D. K., Santra, M., Mann, D. M., McQuillan, D. J., Wong, A. J., and Iozzo, R. V. (1998) Decorin suppresses tumor cell growth by activating the epidermal growth factor receptor. *J. Clin. Investig.* **101,** 406–412
44. Csordás, G., Santra, M., Reed, C. C., Eichstetter, I., McQuillan, D. J., Gross, D., Nugent, M. A., Hajnóczky, G., and Iozzo, R. V. (2000) Sustained down-regulation of the epidermal growth factor receptor by decorin. A mechanism for controlling tumor growth *in vivo*. *J. Biol. Chem.* **275,** 32879–32887
45. Santra, M., Reed, C. C., and Iozzo, R. V. (2002) Decorin binds to a narrow region of the epidermal growth factor (EGF) receptor, partially overlapping but distinct from the EGF-binding epitope. *J. Biol. Chem.* **277,** 35671–35681
46. Santra, M., Eichstetter, I., and Iozzo, R. V. (2000) An anti-oncogenic role for decorin. Down-regulation of ErbB2 leads to growth suppression and cytodifferentiation of mammary carcinoma cells. *J. Biol. Chem.* **275,** 35153–35161
47. Santra, M., Skorski, T., Calabretta, B., Lattime, E. C., and Iozzo, R. V. (1995) *De novo* decorin gene expression suppresses the malignant phenotype in human colon cancer cells. *Proc. Natl. Acad. Sci. U.S.A.* **92,** 7016–7020

48. De Luca, A., Santra, M., Baldi, A., Giordano, A., and Iozzo, R. V. (1996) Decorin-induced growth suppression is associated with up-regulation of p21, an inhibitor of cyclin-dependent kinases. *J. Biol. Chem.* **271,** 18961–18965
49. Santra, M., Mann, D. M., Mercer, E. W., Skorski, T., Calabretta, B., and Iozzo, R. V. (1997) Ectopic expression of decorin protein core causes a generalized growth suppression in neoplastic cells of various histogenetic origin and requires endogenous p21, an inhibitor of cyclin-dependent kinases. *J. Clin. Invest.* **100,** 149–157
50. Patel, S., Santra, M., McQuillan, D. J., Iozzo, R. V., and Thomas, A. P. (1998) Decorin activates the epidermal growth factor receptor and elevates cytosolic Ca^{2+} in A431 carcinoma cells. *J. Biol. Chem.* **273,** 3121–3124
51. Goldoni, S., Humphries, A., Nyström, A., Sattar, S., Owens, R. T., McQuillan, D. J., Ireton, K., and Iozzo, R. V. (2009) Decorin is a novel antagonistic ligand of the Met receptor. *J. Cell Biol.* **185,** 743–754
52. Buraschi, S., Pal, N., Tyler-Rubinstein, N., Owens, R. T., Neill, T., and Iozzo, R. V. (2010) Decorin antagonizes Met receptor activity and down-regulates β-catenin and Myc levels. *J. Biol. Chem.* **285,** 42075–42085
53. Zhu, J. X., Goldoni, S., Bix, G., Owens, R. T., McQuillan, D. J., Reed, C. C., and Iozzo, R. V. (2005) Decorin evokes protracted internalization and degradation of the epidermal growth factor receptor via caveolar endocytosis. *J. Biol. Chem.* **280,** 32468–32479
54. Kermorgant, S., and Parker, P. J. (2005) c-Met signaling. Spatio-temporal decisions. *Cell Cycle* **4,** 352–355
55. Liu, Z. X., Yu, C. F., Nickel, C., Thomas, S., and Cantley, L. G. (2002) Hepatocyte growth factor induces ERK-dependent paxillin phosphorylation and regulates paxillin-focal adhesion kinase association. *J. Biol. Chem.* **277,** 10452–10458
56. Iozzo, R. V., Chakrani, F., Perrotti, D., McQuillan, D. J., Skorski, T., Calabretta, B., and Eichstetter, I. (1999) Cooperative action of germ-line mutations in decorin and p53 accelerates lymphoma tumorigenesis. *Proc. Natl. Acad. Sci. U.S.A.* **96,** 3092–3097
57. Bi, X., Tong, C., Dockendorff, A., Bancroft, L., Gallagher, L., Guzman, G., Iozzo, R. V., Augenlicht, L. H., and Yang, W. (2008) Genetic deficiency of decorin causes intestinal tumor formation through disruption of intestinal cell maturation. *Carcinogenesis* **29,** 1435–1440
58. Reed, C. C., Gauldie, J., and Iozzo, R. V. (2002) Suppression of tumorigenicity by adenovirus-mediated gene transfer of decorin. *Oncogene* **21,** 3688–3695
59. Tralhão, J. G., Schaefer, L., Micegova, M., Evaristo, C., Schönherr, E., Kayal, S., Veiga-Fernandes, H., Danel, C., Iozzo, R. V., Kresse, H., and Lemarchand, P. (2003) *In vivo* selective and distant killing of cancer cells using adenovirus-mediated decorin gene transfer. *FASEB J.* **17,** 464–466
60. Reed, C. C., Waterhouse, A., Kirby, S., Kay, P., Owens, R. T., McQuillan, D. J., and Iozzo, R. V. (2005) Decorin prevents metastatic spreading of breast cancer. *Oncogene* **24,** 1104–1110
61. Seidler, D. G., Goldoni, S., Agnew, C., Cardi, C., Thakur, M. L., Owens, R. T., McQuillan, D. J., and Iozzo, R. V. (2006) Decorin protein core inhibits *in vivo* cancer growth and metabolism by hindering epidermal growth factor receptor function and triggering apoptosis via caspase-3 activation. *J. Biol. Chem.* **281,** 26408–26418
62. Zafiropoulos, A., Nikitovic, D., Katonis, P., Tsatsakis, A., Karamanos, N. K., and Tzanakakis, G. N. (2008) Decorin-induced growth inhibition is overcome through protracted expression and activation of epidermal growth factor receptors in osteosarcoma cells. *Mol. Cancer Res.* **6,** 785–794
63. Goldoni, S., Seidler, D. G., Heath, J., Fassan, M., Baffa, R., Thakur, M. L., Owens, R. T., McQuillan, D. J., and Iozzo, R. V. (2008) An antimetastatic role for decorin in breast cancer. *Am. J. Pathol.* **173,** 844–855
64. Li, X., Pennisi, A., and Yaccoby, S. (2008) Role of decorin in the antimyeloma effects of osteoblasts. *Blood* **112,** 159–168
65. Hu, Y., Sun, H., Owens, R. T., Wu, J., Chen, Y. Q., Berquin, I. M., Perry, D., O'Flaherty, J. T., and Edwards, I. J. (2009) Decorin suppresses prostate tumor growth through inhibition of epidermal growth factor and androgen receptor pathways. *Neoplasia* **11,** 1042–1053
66. Nelimarkka, L., Kainulainen, V., Schönherr, E., Moisander, S., Jortikka, M., Lammi, M., Elenius, K., Jalkanen, M., and Järveläinen, H. (1997) Expression of small extracellular chondroitin/dermatan sulfate proteoglycans is differentially regulated in human endothelial cells. *J. Biol. Chem.* **272,** 12730–12737
67. Nelimarkka, L., Salminen, H., Kuopio, T., Nikkari, S., Ekfors, T., Laine, J., Pelliniemi, L., and Järveläinen, H. (2001) Decorin is produced by capillary endothelial cells in inflammation-associated angiogenesis. *Am. J. Pathol.* **158,** 345–353
68. Schönherr, E., Levkau, B., Schaefer, L., Kresse, H., and Walsh, K. (2001) Decorin-mediated signal transduction in endothelial cells. Involvement of Akt/protein kinase B in up-regulation of p21(WAF1/CIP1) but not p27(KIP1). *J. Biol. Chem.* **276,** 40687–40692
69. Schönherr, E., Sunderkötter, C., Schaefer, L., Thanos, S., Grässel, S., Oldberg, A., Iozzo, R. V., Young, M. F., and Kresse, H. (2004) Decorin deficiency leads to impaired angiogenesis in injured mouse cornea. *J. Vasc. Res.* **41,** 499–508
70. Kinsella, M. G., Fischer, J. W., Mason, D. P., and Wight, T. N. (2000) Retrovirally mediated expression of decorin by macrovascular endothelial cells. Effects on cellular migration and fibronectin fibrillogenesis *in vitro*. *J. Biol. Chem.* **275,** 13924–13932
71. Davies Cde, L., Melder, R. J., Munn, L. L., Mouta-Carreira, C., Jain, R. K., and Boucher, Y. (2001) Decorin inhibits endothelial migration and tube-like structure formation. Role of thrombospondin-1. *Microvasc. Res.* **62,** 26–42
72. Mohan, R. R., Tovey, J. C., Sharma, A., Schultz, G. S., Cowden, J. W., and Tandon, A. (2011) Targeted decorin gene therapy delivered with adeno-associated virus effectively retards corneal neovascularization *in vivo*. *PLoS ONE* **6,** e26432
73. Grant, D. S., Yenisey, C., Rose, R. W., Tootell, M., Santra, M., and Iozzo, R. V. (2002) Decorin suppresses tumor cell-mediated angiogenesis. *Oncogene* **21,** 4765–4777
74. Salomäki, H. H., Sainio, A. O., Söderström, M., Pakkanen, S., Laine, J., and Järveläinen, H. T. (2008) Differential expression of decorin by human malignant and benign vascular tumors. *J. Histochem. Cytochem.* **56,** 639–646
75. Lai, A. Z., Abella, J. V., and Park, M. (2009) Cross-talk in Met receptor oncogenesis. *Trends Cell Biol.* **19,** 542–551
76. Grant, D. S., Kleinman, H. K., Goldberg, I. D., Bhargava, M. M., Nickoloff, B. J., Kinsella, J. L., Polverini, P., and Rosen, E. M. (1993) Scatter factor induces blood vessel formation *in vivo*. *Proc. Natl. Acad. Sci. U.S.A.* **90,** 1937–1941
77. Zhang, Y. W., Su, Y., Volpert, O. V., and Vande Woude, G. F. (2003) Hepatocyte growth factor/scatter factor mediates angiogenesis through positive VEGF and negative thrombospondin 1 regulation. *Proc. Natl. Acad. Sci. U.S.A.* **100,** 12718–12723
78. Chiavarina, B., Whitaker-Menezes, D., Migneco, G., Martinez-Outschoorn, U. E., Pavlides, S., Howell, A., Tanowitz, H. B., Casimiro, M. C., Wang, C., Pestell, R. G., Grieshaber, P., Caro, J., Sotgia, F., and Lisanti, M. P. (2010) HIF1-α functions as a tumor promoter in cancer-associated fibroblasts, and as a tumor suppressor in breast cancer cells. Autophagy drives compartment-specific oncogenesis. *Cell Cycle* **9,** 3534–3551
79. Cohen, I. R., Murdoch, A. D., Naso, M. F., Marchetti, D., Berd, D., and Iozzo, R. V. (1994) Abnormal expression of perlecan proteoglycan in metastatic melanomas. *Cancer Res.* **54,** 5771–5774
80. Iozzo, R. V. (1994) Perlecan. A gem of a proteoglycan. *Matrix Biol.* **14,** 203–208
81. Goyal, A., Pal, N., Concannon, M., Paul, M., Doran, M., Poluzzi, C., Sekiguchi, K., Whitelock, J. M., Neill, T., and Iozzo, R. V. (2011) Endorepellin, the angiostatic module of perlecan, interacts with both the $\alpha2\beta1$ integrin and vascular endothelial growth factor receptor 2 (VEGFR2). A dual receptor antagonism. *J. Biol. Chem.* **286,** 25947–25962
82. Zoeller, J. J., McQuillan, A., Whitelock, J., Ho, S. Y., and Iozzo, R. V. (2008) A central function for perlecan in skeletal muscle and cardiovascular development. *J. Cell Biol.* **181,** 381–394
83. Iozzo, R. V., Buraschi, S., Genua, M., Xu, S. Q., Solomides, C. C., Peiper, S. C., Gomella, L. G., Owens, R. C., and Morrione, A. (2011) Decorin antagonizes IGF receptor I (IGF-IR) function by interfering with IGF-IR activity and attenuating downstream signaling. *J. Biol. Chem.* **286,** 34712–34721

84. Hembry, R. M., Atkinson, S. J., and Murphy, G. (2007) Assessment of gelatinase expression and activity in articular cartilage. *Methods Mol. Med.* **135,** 227–238
85. Okawa, T., Michaylira, C. Z., Kalabis, J., Stairs, D. B., Nakagawa, H., Andl, C. D., Johnstone, C. N., Klein-Szanto, A. J., El-Deiry, W. S., Cukierman, E., Herlyn, M., and Rustgi, A. K. (2007) The functional interplay between EGFR overexpression, hTERT activation, and p53 mutation in esophageal epithelial cells with activation of stromal fibroblasts induces tumor development, invasion, and differentiation. *Genes Dev.* **21,** 2788–2803
86. Liau, S. S., Jazag, A., and Whang, E. E. (2006) HMGA1 is a determinant of cellular invasiveness and *in vivo* metastatic potential in pancreatic adenocarcinoma. *Cancer Res.* **66,** 11613–11622
87. Bourboulia, D., and Stetler-Stevenson, W. G. (2010) Matrix metalloproteinases (MMPs) and tissue inhibitors of metalloproteinases (TIMPs). Positive and negative regulators in tumor cell adhesion. *Semin. Cancer Biol.* **20,** 161–168
88. Woodfin, A., Voisin, M. B., and Nourshargh, S. (2007) PECAM-1, a multifunctional molecule in inflammation and vascular biology. *Arterioscler. Thromb. Vasc. Biol.* **27,** 2514–2523
89. Semenza, G. (2002) Signal transduction to hypoxia-inducible factor 1. *Biochem. Pharmacol.* **64,** 993–998
90. Avraamides, C. J., Garmy-Susini, B., and Varner, J. A. (2008) Integrins in angiogenesis and lymphangiogenesis. *Nat. Rev. Cancer* **8,** 604–617
91. Daum, G., Grabski, A., and Reidy, M. A. (2009) Sphingosine 1-phosphate. A regulator of arterial lesions. *Arterioscler. Thromb. Vasc. Biol.* **29,** 1439–1443
92. Rangel, R., Sun, Y., Guzman-Rojas, L., Ozawa, M. G., Sun, J., Giordano, R. J., Van Pelt, C. S., Tinkey, P. T., Behringer, R. R., Sidman, R. L., Arap, W., and Pasqualini, R. (2007) Impaired angiogenesis in aminopeptidase N-null mice. *Proc. Natl. Acad. Sci. U.S.A.* **104,** 4588–4593
93. Bernabeu, C., Lopez-Novoa, J. M., and Quintanilla, M. (2009) The emerging role of TGF-β superfamily coreceptors in cancer. *Biochim. Biophys. Acta* **1792,** 954–973
94. Hynes, R. O. (2007) *J. Thromb. Haemost.* **5,** Suppl. 1, 32–40
95. Armstrong, L. C., and Bornstein, P. (2003) Thrombospondins 1 and 2 function as inhibitors of angiogenesis. *Matrix Biol.* **22,** 63–71
96. Zhang, X., and Lawler, J. (2007) Thrombospondin-based antiangiogenic therapy. *Microvasc. Res.* **74,** 90–99
97. Pagès, G., and Pouysségur, J. (2005) Transcriptional regulation of the vascular endothelial growth factor gene. A concert of activating factors. *Cardiovasc. Res.* **65,** 564–573
98. Lando, D., Peet, D. J., Whelan, D. A., Gorman, J. J., and Whitelaw, M. L. (2002) Asparagine hydroxylation of the HIF transactivation domain a hypoxic switch. *Science* **295,** 858–861
99. Semenza, G. L. (2009) Regulation of cancer cell metabolism by hypoxia-inducible factor 1. *Semin. Cancer Biol.* **19,** 12–16
100. Easwaran, V., Lee, S. H., Inge, L., Guo, L., Goldbeck, C., Garrett, E., Wiesmann, M., Garcia, P. D., Fuller, J. H., Chan, V., Randazzo, F., Gundel, R., Warren, R. S., Escobedo, J., Aukerman, S. L., Taylor, R. N., and Fantl, W. J. (2003) β-Catenin regulates vascular endothelial growth factor expression in colon cancer. *Cancer Res.* **63,** 3145–3153
101. Milanini-Mongiat, J., Pouysségur, J., and Pagès, G. (2002) Identification of two Sp1 phosphorylation sites for p42/p44 mitogen-activated protein kinases. Their implication in vascular endothelial growth factor gene transcription. *J. Biol. Chem.* **277,** 20631–20639
102. Rasola, A., Fassetta, M., De Bacco, F., D'Alessandro, L., Gramaglia, D., Di Renzo, M. F., and Comoglio, P. M. (2007) A positive feedback loop between hepatocyte growth factor receptor and β-catenin sustains colorectal cancer cell invasive growth. *Oncogene* **26,** 1078–1087
103. Iozzo, R. V., and Schaefer, L. (2010) Proteoglycans in health and disease. Novel regulatory signaling mechanisms evoked by the small leucine-rich proteoglycans. *FEBS J.* **277,** 3864–3875
104. Whitelock, J. M., Murdoch, A. D., Iozzo, R. V., and Underwood, P. A. (1996) The degradation of human endothelial cell-derived perlecan and release of bound basic fibroblast growth factor by stromelysin, collagenase, plasmin, and heparanases. *J. Biol. Chem.* **271,** 10079–10086
105. Goldoni, S., and Iozzo, R. V. (2008) Tumor microenvironment. Modulation by decorin and related molecules harboring leucine-rich tandem motifs. *Int. J. Cancer* **123,** 2473–2479
106. Lee, S., Jilani, S. M., Nikolova, G. V., Carpizo, D., and Iruela-Arispe, M. L. (2005) Processing of VEGF-A by matrix metalloproteinases regulates bioavailability and vascular patterning in tumors. *J. Cell Biol.* **169,** 681–691
107. Wu, B., Crampton, S. P., and Hughes, C. C. (2007) Wnt signaling induces matrix metalloproteinase expression and regulates T cell transmigration. *Immunity* **26,** 227–239
108. Zarrabi, K., Dufour, A., Li, J., Kuscu, C., Pulkoski-Gross, A., Zhi, J., Hu, Y., Sampson, N. S., Zucker, S., and Cao, J. (2011) Inhibition of matrix metalloproteinase 14 (MMP-14)-mediated cancer cell migration. *J. Biol. Chem.* **286,** 33167–33177
109. Gialeli, C., Theocharis, A. D., and Karamanos, N. K. (2011) Roles of matrix metalloproteinases in cancer progression and their pharmacological targeting. *FEBS J.* **278,** 16–27
110. Fata, J. E., Leco, K. J., Voura, E. B., Yu, H. Y., Waterhouse, P., Murphy, G., Moorehead, R. A., and Khokha, R. (2001) Accelerated apoptosis in the Timp-3-deficient mammary gland. *J. Clin. Invest.* **108,** 831–841
111. Bachman, K. E., Herman, J. G., Corn, P. G., Merlo, A., Costello, J. F., Cavenee, W. K., Baylin, S. B., and Graff, J. R. (1999) Methylation-associated silencing of the tissue inhibitor of metalloproteinase-3 gene suggest a suppressor role in kidney, brain, and other human cancers. *Cancer Res.* **59,** 798–802
112. Barski, D., Wolter, M., Reifenberger, G., and Riemenschneider, M. J. (2010) Hypermethylation and transcriptional down-regulation of the *TIMP3* gene is associated with allelic loss on 22q12.3 and malignancy in meningiomas. *Brain Pathol.* **20,** 623–631
113. Zöchbauer-Müller, S., Fong, K. M., Virmani, A. K., Geradts, J., Gazdar, A. F., and Minna, J. D. (2001) Aberrant promoter methylation of multiple genes in non-small cell lung cancers. *Cancer Res.* **61,** 249–255
114. Nath, D., Williamson, N. J., Jarvis, R., and Murphy, G. (2001) Shedding of c-Met is regulated by cross-talk between a G-protein coupled receptor and the EGF receptor and is mediated by a TIMP-3-sensitive metalloproteinase. *J. Cell Sci.* **114,** 1213–1220
115. Hahn, W. C., and Weinberg, R. A. (2002) Rules for making human tumor cells. *N. Engl. J. Med.* **347,** 1593–1603
116. Riggins, K. S., Mernaugh, G., Su, Y., Quaranta, V., Koshikawa, N., Seiki, M., Pozzi, A., and Zent, R. (2010) MT1-MMP-mediated basement membrane remodeling modulates renal development. *Exp. Cell Res.* **316,** 2993–3005
117. Tikhonenko, A. T., Black, D. J., and Linial, M. L. (1996) Viral Myc oncoproteins in infected fibroblasts down-modulate thrombospondin-1, a possible tumor suppressor gene. *J. Biol. Chem.* **271,** 30741–30747
118. Ngo, C. V., Gee, M., Akhtar, N., Yu, D., Volpert, O., Auerbach, R., and Thomas-Tikhonenko, A. (2000) *Cell Growth & Differ.* **11,** 201–210
119. Watnick, R. S., Cheng, Y. N., Rangarajan, A., Ince, T. A., and Weinberg, R. A. (2003) Ras modulates Myc activity to repress thrombospondin-1 expression and increase tumor angiogenesis. *Cancer Cell* **3,** 219–231
120. Santra, M., Santra, S., Zhang, J., and Chopp, M. (2008) Ectopic decorin expression up-regulates VEGF expression in mouse cerebral endothelial cells via activation of the transcription factors Sp1, HIF-1α, and Stat3. *J. Neurochem.* **105,** 324–337
121. Khan, G. A., Girish, G. V., Lala, N., Di Guglielmo, G. M., and Lala, P. K. (2011) Decorin is a novel VEGFR-2-binding antagonist for the human extravillous trophoblast. *Mol. Endocrinol.* **25,** 1431–1443